

Heavy Meson Semileptonic Form Factors from Lattice Quantum Chromodynamics

Euan McLean

Supervised by Prof. Christine Davies

*Submitted in fulfillment of the requirements for the degree of
Doctor of Philosophy*

April 2019



*The University of Glasgow
College of Science and Engineering*

Declaration of originality

This thesis is my own work, except where explicit attribution to others is made. In particular Chapters ... are based on the following publications:

All results and figures presented in these chapters are my own, except for ...

'Part of being a winner is knowing when enough is enough. Sometimes you have to give up the fight and walk away, and move on to something that's more productive.'

- Donald Trump

Acknowledgments

I claim sole credit for everything in this thesis.

Contents

1	Introduction	1
2	Background and Motivation	3
2.1	Testing the Standard Model	3
2.2	Flavour-Changing Charged Currents	5
2.2.1	The CKM Matrix	7
2.2.2	Weak Decays	10
2.2.3	$ V_{cb} $	15
2.2.4	Flavour Anomalies	17
3	Heavy \rightarrow Heavy Meson Semileptonic Decays	21
3.1	Strong Interaction Physics	21
3.1.1	Quantum Chromodynamics	21
3.1.2	Chiral Symmetry	23
3.2	Heavy Quark Physics	27
3.2.1	HQET	27
3.2.2	NRQCD	33
3.3	Form Factors	35
3.3.1	Analyticity	36
3.3.2	Parameterisations	36
3.4	Experimental Status	36
4	Lattice Quantum Chromodynamics	37
4.1	Lattice Gauge Fields	38
4.1.1	The Wilson Gauge Action	38
4.1.2	Improvements	38
4.2	Lattice Fermions	38
4.2.1	The Doubling Problem	39
4.2.2	Staggered Quarks	40
4.2.3	Highly Improved Staggered Quarks	42
4.3	Dealing with Heavy Quarks	43
4.3.1	Heavy HISQ	44
4.3.2	Lattice NRQCD	44

5	Lattice Calculations	45
5.1	Correlation Functions from Lattice Simulations	45
5.1.1	The Path Integral and Generation of Gauge Ensembles	46
5.1.2	Dirac Operator Inversion	46
5.1.3	Staggered Correlation Functions	46
5.2	Analysis of Correlation Functions	50
5.2.1	Non-Linear Regression	51
5.2.2	The Golden Window	55
5.3	Renormalization of Currents	56
5.3.1	Non-perturbative Renormalization of HISQ Currents	58
5.3.2	Matching NRQCD currents to \overline{MS}	58
6	b-Physics from Lattice NRQCD	59
6.1	$B_{(s)} \rightarrow D_{(s)} l \nu$ Form Factors	59
6.1.1	Calculation Setup	59
6.1.2	Results	59
6.1.3	The Subleading Current Problem	59
6.2	Nonperturbative Renormalisation	59
6.2.1	Relativistic Normalisation of the $b \rightarrow c$ Axial Current	59
6.2.2	$b \rightarrow c$ Vector Current Matching to Heavy-HISQ	59
7	$B_s \rightarrow D_s^* l \nu$ Axial Form Factor at Zero Recoil from Heavy-HISQ	61
7.1	Calculation Setup	61
7.2	Results	61
7.3	Implications for $B \rightarrow D^* l \nu$ and $ V_{cb} $	61
8	$B_s \rightarrow D_s l \nu$ Form Factor at All Physical q^2 from Heavy-HISQ	63
8.1	Calculation Setup	63
8.2	Results	63
8.3	HQET low energy constants	63

Introduction

As the LHC continuously refuses to supply new resonances, the high energy physics community places their hope in the intensity frontier to finally break the standard model. Subtle differences between experimental measurements and standard model predictions are the new rock and roll. As collider experiments collect more data and measurements become more precise, theorists must keep up the pace and improve our predictions. What else but Lattice QCD could answer the call of providing first-principle calculations of non-perturbative quantities?

This thesis focuses on the study of calculating form factors for semileptonic $b \rightarrow c$ transitions. These transitions occur between hadrons, bound together by QCD. At the confinement scale ($\sim 1\text{GeV}$), perturbation theory breaks down due to asymptotic freedom, and the only sensible option is to compute the path integral directly.

The b quark is difficult to deal with on the lattice, due to its mass being beyond the momentum cutoff imposed by computationally feasible lattice spacings. I calculate $b \rightarrow c$ form factors using two approaches to dealing with the heavy b , one employing a non-relativistic action for the b (*NRQCD*), and the other relying on heavy quark effective theory to extrapolate upwards to the b mass (*Heavy-HISQ*). The main take-home from this thesis is the following: **NRQCD is on shaky ground, and Heavy-HISQ is an excellent way to live.**

Using NRQCD, I attempted to compute form factors for the $B_{(s)} \rightarrow D_{(s)} l \nu$ decays. The depletion of the signal/noise ratio in correlation functions featuring high spacial momentum means lattice data for this decay was limited to the high q^2 region.

In NRQCD, flavour-changing current operators are made of an infinite series

of terms in powers of the b -quark velocity v , each requiring their own normalisation via perturbative matching to continuum QCD. It was discovered during this work that subleading terms in this series, that were originally thought to be negligible, in fact may be an important contribution. Since the perturbative matching calculations for these terms have not been performed, this caused a somewhat insurmountable obstacle for the NRQCD approach to calculating $b \rightarrow c$ form factors.

The NRQCD approach could in principle be saved by finding non-perturbative normalizations of these large subleading pieces of the current. We investigated a way of achieving this by comparing NRQCD lattice data to pre-existing and more reliable Heavy-HISQ lattice data, with limited success.

To sidestep the problems with NRQCD, We adopted a totally new approach: the Heavy-HISQ approach. With this, we successfully calculated the $B_s \rightarrow D_s^* l \nu$ axial form factor at zero recoil. This demonstrated the power of the heavy-HISQ approach, and laid the groundwork for a study of $B_s \rightarrow D_s^* l \nu$ form factors away from zero recoil and $B \rightarrow D^* l \nu$ form factors. We also calculated $B_s \rightarrow D_s l \nu$ form factors throughout the full physical range of momentum transfer. These studies, when combined with future experimental data of the $B_s \rightarrow D_s l \nu$ and $B_s \rightarrow D_s^* l \nu$ decays, will supply new tests of the standard model, and new channels to determining the CKM parameter $|V_{cb}|$.

All work reported in this thesis was performed using gluon ensembles courtesy of the MILC collaboration, accounting for dynamical up, down, strange and charm HISQ quarks in the sea. We computed correlation functions using a combination of the MILC code, and HPQCD's NRQCD code.

Background and Motivation

In this chapter I lay out the physics context of my work. We will define the framework we are testing, the standard model. We will expand on the details of the specific sector we are interested in - the flavour sector and the CKM matrix.

2.1 Testing the Standard Model

need to add: intro to discrete Lorentz symmetries

mention how $SU(3)_C \times SU(2)_L \times U(1)_Y$ relates to electromagnetism via EWSB.

include any stuff in Lenz's flavour physics lectures intro to SM that has been missed out here.

maybe put QCD section in here, before the FCCC section (since I claim that QCD matrix elements cannot be computed with perturbation theory...)

READING LIST: Lenz, Flavour physics lectures. 1812.11211, 1703.08170

'The B-physics program' :<https://www.ncbi.nlm.nih.gov/pmc/articles/PMC4737432/#andp2015002sec-0020title>

The Standard Model of Particle Physics (SM) is, so far, the most successful theory for describing fundamental particles and their interactions. It is an effective Yang-Mills quantum field theory. It is most succinctly defined by listing it's symmetries, field content, and the irreducible representations (irreps) of the symmetries that those fields transform under.

The symmetries are the following. The Lorentz group $SO(3,1)$, the group of coordinate transformations that leave the Minkowski metric invariant, which can be decomposed into $SU(2)_l \times SU(2)_r$ (*left-handed* and *right-handed*). We denote an irrep as (a, b) where a is the σ^z eigenvalue under $SU(2)_l$ transforms, and b is that of $SU(2)_r$. Then there are internal local gauge symmetries:

$$SU(3)_C \times SU(2)_L \times U(1)_Y, \quad (2.1)$$

irreps of which we denote with (x, y, z) , where x, y are the $SU(3)_C$ and $SU(2)_W$ irreps and z is the charge under $U(1)_Y$.

The field content is: gauge bosons for each generator of the above gauge symmetries, each transforming in the adjoint of their corresponding symmetry and in the $(1/2, 1/2)$ irrep of the Lorentz group, denoted B_μ , W_μ , G_μ respectively. There are 6 $SU(2)_L$ doublets in the $(1/2, 0)$ Lorentz irrep;

$$Q_{1,2,3} = \begin{pmatrix} u_L \\ d_L \end{pmatrix}, \begin{pmatrix} c_L \\ s_L \end{pmatrix}, \begin{pmatrix} t_L \\ b_L \end{pmatrix} \quad , \quad (\mathbf{3}, \mathbf{2}, 1/6) \quad (2.2)$$

$$L_{1,2,3} = \begin{pmatrix} \nu_{e,L} \\ e_L \end{pmatrix}, \begin{pmatrix} \nu_{\mu,L} \\ \mu_L \end{pmatrix}, \begin{pmatrix} \nu_{\tau,L} \\ \tau_L \end{pmatrix} \quad , \quad (\mathbf{1}, \mathbf{2}, -1) \quad (2.3)$$

and 9 $SU(2)_W$ singlets in the $(0, 1/2)$ Lorentz irrep;

$$u_{1,2,3}^R = u_R, c_R, t_R \quad , \quad (\bar{\mathbf{3}}, \mathbf{1}, 2/3) \quad (2.4)$$

$$d_{1,2,3}^R = d_R, s_R, b_R \quad , \quad (\bar{\mathbf{3}}, \mathbf{1}, -1/3) \quad (2.5)$$

$$e_{1,2,3}^R = e_R, \mu_R, \tau_R \quad , \quad (\mathbf{1}, \mathbf{1}, -1) \quad (2.6)$$

We have also listed the SM gauge irreps next to each definition. There is also in principle a further set of right-handed $SU(2)_L$ singlets, $\nu_{1,2,3}^R = (\nu_{e,R}, \nu_{\mu,R}, \nu_{\tau,R})$, but these are singlets of the entire SM gauge group so in a phenomenological sense very much 'not there'. There is also a Lorentz scalar $SU(2)_L$ doublet, the Higgs H , with in Gauge irrep $(1, 2, 1/2)$ that obtains a vacuum expectation value and causes a breaking of the above gauge group, described in the next section.

There is at present no confirmed evidence of physics beyond the SM (or *new physics* (NP)), besides the presence of neutrino (ν) masses. However, there are a number of problems with the SM that heavily imply that there must be new physics. Among the most famous sources of concern are:

- **Dark Matter & Dark Energy** - an estimated 96% of the content of the universe is dark matter and dark energy, that does not interact with the SM gauge group (only via gravity), so cannot be explained by the SM.
- **Matter/Antimatter Asymmetry** - the SM requires there to be an equal amount of matter and antimatter in the universe, however, we observe a massive dominance of matter over antimatter.
- **Neutrino Oscillations** - different species of neutrinos oscillate into each other over time, there is no SM mechanism to explain this.

- **The Hierarchy Problem** - the SM is 'finely tuned', the chances of the Higgs choosing it's current vacuum expectation value is estimated to be one in $\sim 10^{45}$.

The central goal of particle physics is currently to pin down evidence against the standard model. Only once we have detailed knowledge of how it breaks down will theorists be able to uniquely determine a new theory of fundamental physics.

There are many promising approaches to achieve this. They are traditionally separated into

- **The Energy Frontier** - explore the highest possible energies reachable with accelerators, directly looking for new physics via the production and identification of new states of matter.
- **The Cosmic Frontier** - use the universe as an experimental laboratory and observatory, taking advantage of naturally occurring events to observe indications of new interactions.
- **The Intensity Frontier** - use intense sources of particles from accelerators, reactors, the sun and the atmosphere to make ultra-precise measurements and find subtle deviations from SM predictions.

The work in this thesis contributes to the third approach. There is a rising tide of more and more SM observables being measured and predicted more and more precisely. It is only a matter of time until one of these observables yields a statistically significant deviation from the SM.

2.2 Flavour-Changing Charged Currents

The SM tests relevant to this work are on quark flavour-changing interactions. Here we will detail the parts of the SM relevant to these interactions.

The $SU(2)_L$ gauge symmetry of the SM is mediated by the vector boson $W = W^1\tau_1 + W^2\tau_2 + W^3\tau_3$, where τ_i are the three $SU(2)$ generators acting on the $SU(2)_L$ doublets defined in the last section. It is convenient to redefine the fields $W = W^+(\tau_0 + i\tau_1) + W^-(\tau_0 - i\tau_1) + W^3\tau_3$. W^\pm, W^3 are the stationary states at low energies due to electroweak symmetry breaking.

The part of the SM lagrangian that describes the coupling of W^\pm to fermions is

given by

$$\mathcal{L}_{\text{FCCC}} = \frac{e}{\sqrt{2} \sin \theta_W} \left(\bar{u}_L^i \not{W}^+ d_L^i + \bar{d}_L^i \not{W}^- u_L^i + \bar{\nu}_L^i \not{W}^+ e_L^i + \bar{e}_L^i \not{W}^- \nu_L^i \right) \quad (2.7)$$

where e is the electron charge, θ_W is the Weinberg angle, and $\not{V} = \gamma^\mu V_\mu$ where γ^μ are members of the Clifford algebra acting on fermion spin components. To understand the interactions these terms cause we must also consider the mass terms for the fermions:

$$\mathcal{L}_{\text{mass}} = y_{ij}^u \left(\frac{v}{\sqrt{2}} \right) u_L^i u_R^j + y_{ij}^d \left(\frac{v}{\sqrt{2}} \right) d_L^i d_R^j + y_{ij}^e \left(\frac{v}{\sqrt{2}} \right) e_L^i e_R^j. \quad (2.8)$$

These terms come from the coupling of the fermions to the Higgs field, where the Higgs has taken a vacuum expectation value v at low energies. $y_{ij}^{u,d,e}$ are the Yukawa matrices, parameterising the coupling of the fermions to the Higgs, consisting of free parameters. The absence of right-handed neutrinos forbids an analogous term for neutrinos.

Due to these non-diagonal mass terms, the fundamental fermion fields are not stationary states. To obtain a more useful representation, one rotates the fields to diagonalise these terms

$$\psi_i^L \rightarrow L_{ij}^\psi \psi_j^L, \quad \psi_R^i \rightarrow R_{ij}^\psi \psi_R^j, \quad (2.9)$$

where $\psi = u, d$ or e , and we fix L_{ij}^ψ, R_{ij}^ψ according to

$$y^\psi \left(\frac{v}{\sqrt{2}} \right) = L^\psi M^\psi R^\psi \quad (2.10)$$

where M^ψ is diagonal. This results in diagonal mass terms, but also has an effect on $\mathcal{L}_{\text{FCCC}}$:

$$\mathcal{L}_{\text{FCCC}} = \frac{e}{\sqrt{2} \sin \theta_W} \left(V_{ij} \bar{u}_L^i \not{W}^+ d_L^j + V_{ij}^* \bar{d}_L^i \not{W}^- u_L^j + \bar{\nu}_L^i \not{W}^+ e_L^i + \bar{e}_L^i \not{W}^- \nu_L^i \right), \quad (2.11)$$

where $V = L^{u\dagger} L^d$ is by construction a unitary matrix ($V^\dagger V = (L^{d\dagger} L^u)(L^{u\dagger} L^d) = L^d L^{d\dagger} = 1$). V is the famous Cabibbo–Kobayashi–Maskawa (CKM) matrix, consisting of parameters that must be fixed by experiment. There is no non-diagonal flavour structure in the last two terms, because we have redefined the neutrino fields: $\nu_L \rightarrow L^{e\dagger} \nu_L$, absorbing the rotation of the e_L fields. This can be done with impunity due to the lack of neutrino mass terms.

Another useful redefinition is to collect the left-handed and right-handed fermion fields into Dirac spinors ψ :

$$\psi = \psi_L + \psi_R, \quad \psi_L = \frac{1}{2} (1 - \gamma^5) \psi, \quad \psi_R = \frac{1}{2} (1 + \gamma^5) \psi \quad (2.12)$$

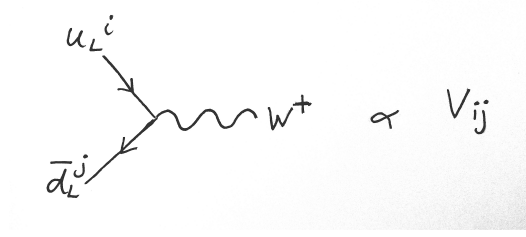


Figure 2.1: The flavour-changing charged current vertex.

In terms of Dirac spinors, $\mathcal{L}_{\text{FCCC}}$ can be written as

$$\mathcal{L}_{\text{FCCC}} = \frac{e}{\sqrt{2} \sin \theta_W} \left(V_{ij} J_\mu^{ij} W^{+\mu} + V_{ij}^* J_\mu^{ij\dagger} W^{-\mu} + L_\mu^{ii} W^{+\mu} + L_\mu^{ii\dagger} W^{-\mu} \right), \quad (2.13)$$

$$L_\mu^{ij} = \frac{1}{2} (\bar{\nu}^i \gamma_\mu e^j - \bar{\nu}^i \gamma_5 \gamma_\mu e^j), \quad (2.14)$$

$$J_\mu^{ij} = \frac{1}{2} (\bar{u}^i \gamma_\mu d^j - \bar{u}^i \gamma_5 \gamma_\mu d^j) \equiv V_\mu^{ij} - A_\mu^{ij}. \quad (2.15)$$

J_μ^{ij} is known as the Flavour-Changing Charged Current (FCCC), elucidating the mysterious naming of the above Lagrangian. It is often broken up into the *vector* and *axial-vector* components, V_μ and A_μ respectively, since these two components can be categorised according to their transformations under the Lorentz group. V_μ is labelled 1^+ , where the 1 represents its total spin, and the + represents its positive parity $P : V_\mu \rightarrow V_\mu$. A_μ is instead labelled 1^- , due to its negative parity $P : A_\mu \rightarrow -A_\mu$.

We can now turn to the physical consequences of $\mathcal{L}_{\text{FCCC}}$. The interactions given in this part of the Lagrangian describe a quark changing flavour while emitting a W^\pm boson.

The propensity for flavour i to decay into another flavour j , is governed in part by energy constraints and in part by the associated CKM element V_{ij} . These interactions at the quark level mediate meson decays, namely leptonic and semileptonic decays, described in section 2.2.2.

2.2.1 The CKM Matrix

The exact values of the CKM matrix elements are of interest in the search for new physics. The CKM matrix is unitary by construction, however, if we were to discover that the values we measure experimentally do not combine to produce a unitary matrix, this would be evidence that the elements we are measuring in fact compose a submatrix of a unitary matrix larger than 3×3 . This would imply the presence of further, heavier quark generations.

Another source of interest in the CKM values is CP violation. CP violation is a global symmetry exhibited by $\mathcal{L}_{\text{SM}} - \mathcal{L}_{\text{FCCC}}$, and physically corresponds to a symmetry between particles and antiparticles. CP violation is one of the famous *Sakharov conditions*, the conditions necessary for a theory to explain the matter/antimatter asymmetry observed in the universe. CP is generically violated when a parameter of the theory has an imaginary component. As will be shown below, the CKM matrix contains one physical phase, making $\mathcal{L}_{\text{FCCC}}$ a source of CP violation. However, the extent of CP violation in the flavour sector is not sufficient to explain the matter/antimatter asymmetry, so the necessary CP violating processes will likely come from new physics beyond the standard model.

To understand the structure of the CKM, we must first ask how many independent physical parameters there are. If one imagines that V is purely real, then it becomes an $SO(3)$ matrix, which can be parameterised by 3 angles, so there are $N_{\text{real}} = 3$ independent real parameters. A member of $SU(3)$ has 9 independent parameters, so there must be $N_{\text{im}} = N - N_{\text{real}} = 6$ independent phases.

However, we have the freedom to remove some of those phases via a redefinition of the quark fields. $\mathcal{L}_{\text{SM}} - \mathcal{L}_{\text{FCCC}}$ has a global $U(1)^6$ symmetry, a rephasing of each of the 6 quark flavours. One can rephase each flavour without modifying $\mathcal{L}_{\text{SM}} - \mathcal{L}_{\text{FCCC}}$, but with the effect of changing V :

$$V \rightarrow \begin{pmatrix} e^{-ia} & 0 & 0 \\ 0 & e^{-ib} & 0 \\ 0 & 0 & e^{-ic} \end{pmatrix} V \begin{pmatrix} e^{id} & 0 & 0 \\ 0 & e^{ie} & 0 \\ 0 & 0 & e^{if} \end{pmatrix}, \quad (2.16)$$

where $a, b, c, d, e, f \in \mathbb{R}$. So perhaps one can tune each of these 6 phases to remove all 6 phases in V . This is not quite right, we in fact only have the ability to remove 5 of the 6 phases. To see why we can redefine the phases in the following way;

$$V \rightarrow \begin{pmatrix} e^{-ia} & 0 & 0 \\ 0 & e^{-i(a+\alpha)} & 0 \\ 0 & 0 & e^{-i(a+\beta)} \end{pmatrix} V \begin{pmatrix} e^{i(a+\gamma)} & 0 & 0 \\ 0 & e^{i(a+\delta)} & 0 \\ 0 & 0 & e^{i(a+\epsilon)} \end{pmatrix}, \quad (2.17)$$

with $\alpha, \beta, \gamma, \delta, \epsilon \in \mathbb{R}$. a is a useless phase - it will always cancel with itself so cannot be used to remove a phase from V . Hence, one can remove 5 of the 6 phases by redefining the quark fields, leaving one physical phase in the CKM matrix.

This can be seen as due to the explicit symmetry breaking property of $\mathcal{L}_{\text{FCCC}}$. Inclusion of $\mathcal{L}_{\text{FCCC}}$ breaks the global $U(1)^6$ symmetry down, $U(1)^6 \rightarrow U(1)$, where the broken symmetry is a rephasing of all of the quark flavours by the same amount.

This says we can modify $\mathcal{L}_{\text{FCCC}}$ by $N_{\text{broken}} = 5$ independent phases without modifying the rest of the Lagrangian.

So the CKM has 3 real parameters and 1 complex phase. A common parameterisation is

$$V = \begin{pmatrix} 1 & 0 & 0 \\ 0 & \cos \theta_{23} & \sin \theta_{23} \\ 0 & -\sin \theta_{23} & \cos \theta_{23} \end{pmatrix} \begin{pmatrix} 1 & 0 & \sin \theta_{12} e^{i\delta} \\ 0 & 1 & 0 \\ -\sin \theta_{13} e^{i\delta} & 0 & \cos \theta_{13} \end{pmatrix} \begin{pmatrix} \cos \theta_{12} & \sin \theta_{12} & 0 \\ -\sin \theta_{12} & \cos \theta_{12} & 0 \\ 0 & 0 & 1 \end{pmatrix}. \quad (2.18)$$

A useful parameterisation for understanding the relative sizes of the CKM elements is due to Wolfenstein. Define the Wolfenstein parameter $\lambda = \sin \theta_{12}$, which is known experimentally to be around $\lambda \simeq 0.22$. Then $\cos \theta_{12} = \sqrt{1 - \sin^2 \theta_{12}} = \sqrt{1 - \lambda^2} \simeq 1 - \lambda^2/2$. Observing then that $\sin \theta_{23} \sim 0.04 \simeq \lambda^2$ and $\sin \theta_{13} \sim 0.004 \simeq \lambda^3/3$, we can write the matrix as

$$V \simeq \begin{pmatrix} 1 - \frac{1}{2}\lambda^2 & \lambda & \frac{1}{3}\lambda^3 e^{i\delta} \\ -\lambda & 1 - \frac{1}{2}\lambda^2 & \lambda^2 \\ \lambda^3(1 - \frac{1}{3}e^{i\delta}) & -\lambda^2 & 1 \end{pmatrix} = \begin{pmatrix} \mathcal{O}(1) & \mathcal{O}(\lambda) & \mathcal{O}(\lambda^3) \\ \mathcal{O}(\lambda) & \mathcal{O}(1) & \mathcal{O}(\lambda^2) \\ \mathcal{O}(\lambda^3) & \mathcal{O}(\lambda^2) & \mathcal{O}(1) \end{pmatrix} \quad (2.19)$$

There is a clear hierarchy between the values - the CKM matrix is close to the unit matrix. Inter-generational mixing is dominant, dropping from second to first generation is suppressed by λ , dropping from third to second by λ^2 , and dropping from third to first by λ^3 . The SM supplies no compelling explanation of why this hierarchy exists, it is expected that new physics beyond the SM will supply some natural explanation.

The assumption of unitarity in V ,

$$V_{ji}^* V_{jk} = \delta_{ik}, \quad (2.20)$$

imposes 9 constraints on the CKM elements. Each of these constraints gives a test of the SM, if one of these constraints is found to be violated, this represents evidence of new physics. The most studied constraint is given by taking $i = 3, k = 1$;

$$\frac{V_{ud}V_{ub}^*}{V_{cd}V_{cb}^*} + \frac{V_{td}V_{tb}^*}{V_{cd}V_{cb}^*} + 1 = 0. \quad (2.21)$$

This can be visualized as a triangle (known as the *unitarity triangle*) on the complex plane, as shown in figure 2.2.

For unitarity, the triangle must close, in other words, $\alpha + \beta + \gamma = \pi/2$. Hence, to test the CKM unitarity experimentalists measure these angles

$$\alpha = \arg \left(-\frac{V_{td}V_{tb}^*}{V_{ud}V_{ub}^*} \right), \beta = \arg \left(-\frac{V_{cd}V_{cb}^*}{V_{td}V_{tb}^*} \right), \gamma = \arg \left(-\frac{V_{ud}V_{ub}^*}{V_{cd}V_{cb}^*} \right). \quad (2.22)$$

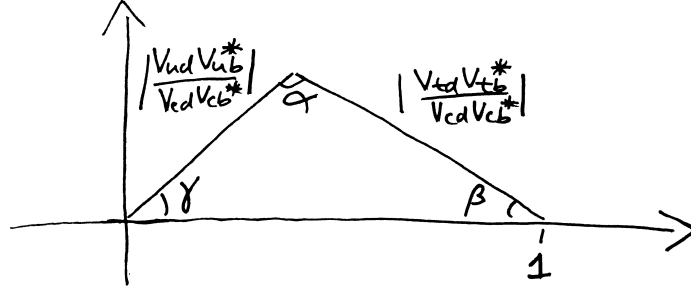


Figure 2.2: A sketch of the unitarity triangle.

The unitarity triangle also contains information about CP-violation from flavour-changing charged currents. The so-called Jarlskog invariant, $J = \sin \theta_{12} \sin \theta_{23} \sin \theta_{31} \cos \theta_{12} \cos \theta_{23} \cos \theta_{31}^2 \sin \delta$, a measure of CP-violation, is proportional to the area enclosed by the triangle.

The most recent PDG update [1] reports the following averages for the measurements of CKM elements;

$$|V| = \begin{pmatrix} 0.97446 \pm 0.00010 & 0.22452 \pm 0.00044 & 0.00365 \pm 0.00012 \\ 0.22438 \pm 0.00044 & 0.97359^{+0.00010}_{-0.00011} & 0.04214 \pm 0.00076 \\ 0.00896^{+0.00024}_{-0.00023} & 0.04133 \pm 0.00074 & 0.999105 \pm 0.000032 \end{pmatrix}. \quad (2.23)$$

The averages given here are consistent with unitarity in all available tests. For example, taking (2.20) with $i = k = 1$, we find $|V_{ud}|^2 + |V_{us}|^2 + |V_{ub}|^2 = 0.9994 \pm 0.0005$. The angles of the unitarity triangle currently satisfy $\alpha + \beta + \gamma = (180 \pm 7)^\circ$.

Increasing the precision of CKM determinations are necessary to provide more stringent tests of CKM unitarity.

2.2.2 Weak Decays

We now move on to the methods of determining CKM elements. At the confinement scale ($\sim 1\text{GeV}$ and below), quarks are confined by QCD in hadrons. At these energies, the dynamics of quarks are only experimentally accessible by probing the dynamics of hadrons. CKM matrix elements are determined by studying hadron decays.

First a word on hadrons. Hadrons are broadly categorized into mesons (charged with one valence quark and one valence antiquark) and baryons (three valence quarks). The entirety of this thesis is concerned with mesons. Mesons are categorized in terms of the flavours they are charged under and their representations

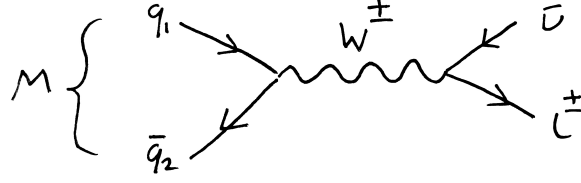


Figure 2.4: Leptonic decay of meson M at tree level in the electroweak coupling.

where D_W is the W^- propagator, $|M\rangle$ is the ground state of the meson M , and $|l\bar{\nu}\rangle$ is a lepton-antineutrino state. We are using the notation $L_\mu^l = L_\mu^{kk}$, where l represents the k th charged lepton. If the momentum of the meson, p^2 , is much smaller than the W mass squared, one can integrate out the dynamics of the W to move into the Fermi effective theory [2];

$$\begin{aligned} \left(\frac{ie}{\sqrt{2}\sin\theta_W}\right)^2 D_W^{\mu\nu}(p^2) &= \left(\frac{ie}{\sqrt{2}\sin\theta_W}\right)^2 \left(\frac{-ig^{\mu\nu}}{p^2 - M_W^2}\right) \\ &= \underbrace{\frac{i}{M_W^2} \left(\frac{ie}{\sqrt{2}\sin\theta_W}\right)^2}_{\equiv -2\sqrt{2}G_F} g^{\mu\nu} + \mathcal{O}\left(\frac{p^2}{M_W^4}\right). \end{aligned} \quad (2.25)$$

Then \mathcal{M} can be factorised;

$$\mathcal{M} \simeq -2\sqrt{2}V_{q_1q_2} \langle l\bar{\nu} | L_\mu^l | \Omega \rangle \langle \Omega | J^{q_1q_2\mu} | M \rangle. \quad (2.26)$$

$\langle \Omega | J_\mu^{q_1q_2} | M \rangle$ is a non-perturbative quantity, since it concerns the transitions of a strongly coupled bound state (QCD at the confinement scale). We know that it has a lorentz index μ , and the only Lorentz vector in the system is the meson's 4-momentum p_μ . So we define

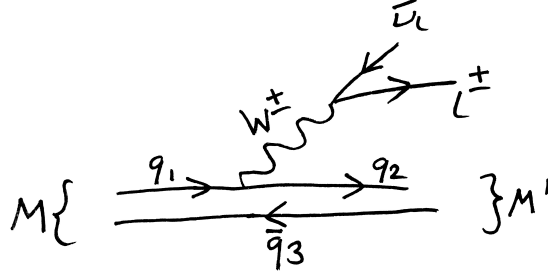
$$\langle \Omega | J_{q_1q_2}^\mu | M \rangle = p^\mu f_M, \quad (2.27)$$

where f_M is a Lorentz invariant known as the *decay constant* of the meson M , and encodes all non-perturbative information in the amplitude.

By taking the modulus squared of \mathcal{M} , and integrating over all allowed momenta of the final state, one finds the decay rate of the process:

$$\Gamma(M \rightarrow l\bar{\nu}) = \frac{G_F^2}{8\pi} f_M^2 m_l^2 M_M \left(1 - \frac{m_l}{M_M}\right)^2 |V_{q_1q_2}|^2, \quad (2.28)$$

In order to find $|V_{q_1q_2}|$, one requires both a measurement of $\Gamma(M \rightarrow l\bar{\nu})$, and a value for f_M . f_M can be computed in a Lattice QCD calculation.

Figure 2.5: Semileptonic decay, $M \rightarrow M' l \bar{\nu}$, at tree level in electroweak coupling.

A similar story accompanies semileptonic decays. At tree level in the electroweak coupling, a typical semileptonic decay is depicted in fig. 3.1. The amplitude is given by

$$\begin{aligned}
 \mathcal{M} &= \left(\frac{ie}{\sqrt{2} \sin \theta_W} \right) V_{q_1 q_2} \langle M', l \bar{\nu} | J_\mu^{q_1 q_2} D_W^{\mu\nu} L_\nu^l | M \rangle \\
 &\simeq -2\sqrt{2} G_F V_{q_1 q_2} \langle M', l \bar{\nu} | J_\mu^{q_1 q_2} L^\mu | M \rangle \\
 &\simeq -2\sqrt{2} G_F V_{q_1 q_2} \langle l \bar{\nu} | L^\mu | \Omega \rangle \langle M' | J_\mu^{q_1 q_2} | M \rangle
 \end{aligned} \tag{2.29}$$

where on the second line we have integrated out the W propagator in using the same expansion as in the leptonic case, and on the third line we have factorised the QCD part from the electroweak part. The matrix element $\langle M' | J_\mu^{q_1 q_2} | M \rangle$ is a non-perturbative quantity. Unlike in the previous case, there are a number of ways one can choose to parameterise this matrix element, and appropriate choices vary depending on the quantum numbers of M and M' . Of interest to us are the cases where M is a pseudoscalar meson 0^- , and M' is either pseudoscalar or vector 1^- .

In the **pseudoscalar** \rightarrow **pseudoscalar** case, only the vector component of the current survives in the matrix element, $\langle M' | J_\mu^{q_1 q_2} | M \rangle = \langle M' | V_\mu^{q_1 q_2} | M \rangle$, $\langle M' | A_\mu^{q_1 q_2} | M \rangle$ vanishes since this does not respect the parity invariance of QCD. The most popular parameterisation of $\langle M' | J_\mu^{q_1 q_2} | M \rangle$ is

$$\langle M' | V_\mu^{q_1 q_2} | M \rangle = f_+(q^2) \left[P_\mu + p_\mu - \frac{M^2 - m^2}{q^2} q_\mu \right] + f_0(q^2) \frac{M^2 - m^2}{q^2} q_\mu \tag{2.30}$$

$f_0(q^2)$ and $f_+(q^2)$, known as the scalar and vector form factors, encode all non-perturbative information. We now have non-perturbative functions of q^2 rather than a single number. q^2 , the momentum carried away from the meson by the W , has an allowed range of values if the final states are on-shell;

$$m_l^2 \leq q^2 \leq (M - m)^2. \tag{2.31}$$

By integrating $|\mathcal{M}|^2$ over all final lepton and neutrino momenta, one finds a differential decay rate.

$$\begin{aligned} \frac{d\Gamma}{dq^2}(M \rightarrow M' l \bar{\nu}) = & \eta_{\text{EW}} \frac{G_F^2 |V_{q_1 q_2}|^2}{24\pi^3 M^2} \left(1 - \frac{m_l^2}{q^2}\right)^2 |\mathbf{p}| \times \\ & \left[\left(1 + \frac{m_l^2}{2q^2}\right) M^2 |\mathbf{p}|^2 f_+^2(q^2) + \frac{3m_l^2}{8q^2} (M^2 - m^2)^2 f_0^2(q^2) \right]. \end{aligned} \quad (2.32)$$

η_{EW} is the electroweak correction, due to diagrams involving an exchange of a photon or a Z -boson alongside the W between the meson and leptons. \mathbf{p} is the final meson state (M') spacial momentum. Once again, to deduce $|V_{q_1 q_2}|$, one requires both the decay rates $d\Gamma/dq^2$, and the form factors $f_0(q^2), f_+(q^2)$. To precisely determine the form factors requires a Lattice QCD calculation.

In the **pseudoscalar** \rightarrow **vector** case, both the vector and axial-vector components of the current survive in the matrix element. A common choice of parameterisation is A common choice of parameterization is

$$\langle M'(\epsilon) | V_{q_1 q_2}^\mu | M \rangle = i\sqrt{Mm} h_V^s(w) \epsilon_{\mu\nu\alpha\beta} \epsilon^{*\nu} v'^\alpha v^\beta, \quad (2.33)$$

$$\begin{aligned} \langle M'(\epsilon) | A_{q_1 q_2}^\mu | M \rangle = & \sqrt{Mm} [h_{A_1}^s(w)(w+1)\epsilon_\mu^* - \\ & h_{A_2}^s(w)\epsilon^* \cdot v v_\mu - h_{A_3}^s(w)\epsilon^* \cdot v v'^\mu]. \end{aligned} \quad (2.34)$$

$v = P/M$ and $v' = p/m$ are the 4-velocities of M and M' respectively. ϵ is the polarization of the vector meson M' . $w = v \cdot v'$ is known as the recoil parameter, this is an alternative to q^2 often used in heavy quark effective theory. $h_V(w), h_{A_0}(q^2), h_{A_1}(q^2)$, and $h_{A_2}(q^2)$ are the form factors accounting for the non-perturbative physics. The decay rate is given by

$$\frac{d\Gamma}{dw}(M \rightarrow M' l \bar{\nu}) = \frac{G_F^2 m^3 |\eta_{\text{EW}} V_{q_1 q_2}|^2}{4\pi^3} (M-m)^2 \sqrt{w^2 - 1} \chi(w) |\mathcal{F}(w)|^2, \quad (2.35)$$

where $\mathcal{F}(w)$ is a linear combination of the form factors, and $\chi(w)$ is a known function of w .

At the zero recoil point, where q^2 is maximized at $q_{\text{max}}^2 = (M-m)^2$, (corresponding to $w = 1$), a single form factor contributes

$$\mathcal{F}(1) = h_{A_1}(1). \quad (2.36)$$

However the differential decay rate vanishes at $w = 1$. A common approach to determine $|V_{q_1 q_2}|$, for example used to find $|V_{cb}|$ via the $B \rightarrow D^* l \bar{\nu}$ decay, is to find $|\mathcal{F}(1) V_{cb}|^2$ at zero recoil by extrapolating from experimental data at non-zero recoil, and combining this with a lattice QCD determination of $h_{A_1}(1)$.

2.2.3 $|V_{cb}|$

The family of weak decays that have attracted the most attention are decays of B mesons (pseudoscalar mesons containing a valence b and u, d, s or c quark). The B meson decays into a rich variety of decay products. It is the heaviest quark flavour that can be found in hadrons. The only heavier quark, the top quark, has a mass far above the confinement scale, so does not feature as a valence quark in hadrons.

The b can decay into either a charm or an up quark via the flavour changing charged current. In this thesis we are interested in the $b \rightarrow c$ transition, with an amplitude proportional to the CKM element $|V_{cb}|$. In this section we give a brief overview of how this is calculated and the value's current status.

B meson decays can be measured in a number of experiments. There are two so-called b -factories, the Belle (II) experiment at the KEKB collider in Japan, and the BaBar experiment at the PEP-II collider at SLAC laboratory in the US. These are e^+e^- colliders, that collide with an energy tuned to the mass of the $\Upsilon(4s)$, an excited state of the Υ meson (a 1^- state with $\bar{b}b$ valence quarks). The $\Upsilon(4s)$ has a large branching fraction into a $B\bar{B}$ pair, the decays of these can be measured with large statistics. B decays can also be measured in proton colliders, like the LHCb experiment at CERN. Measurements from LHCb have poorer statistics but cover a larger range of the phase space of final states, due to the variance of momenta in the initial state protons.

So far 3 approaches to determining $|V_{cb}|$ have been carried out.

- $B \rightarrow D^* l \bar{\nu}$ decay rate measurements are extrapolated to zero recoil to determine $|V_{cb} h_{A_1}(1)|$. Then dividing out $h_{A_1}(1)$ from a Lattice calculation, one finds $|V_{cb}|$.
- $B \rightarrow D l \bar{\nu}$ decay rates are measured throughout q^2 , and combined with $f_0(q^2)$ and $f_+(q^2)$ from lattice calculations.
- $B \rightarrow X_c l \bar{\nu}$ decay rates are measured (where X_c is all possible charmed final state mesons), this is used to constrain elements in the operator product expansion, a method first devised in [3, 4].

The first two are referred to as *exclusive* and the third *inclusive*. A selection of the most accurate examples of each method of determination is given in figure 2.6.

This tells a story of the recent history of $|V_{cb}|$. Determinations from $B \rightarrow D l \bar{\nu}$ have been consistent but not as precise as via the other two methods. Until recently,

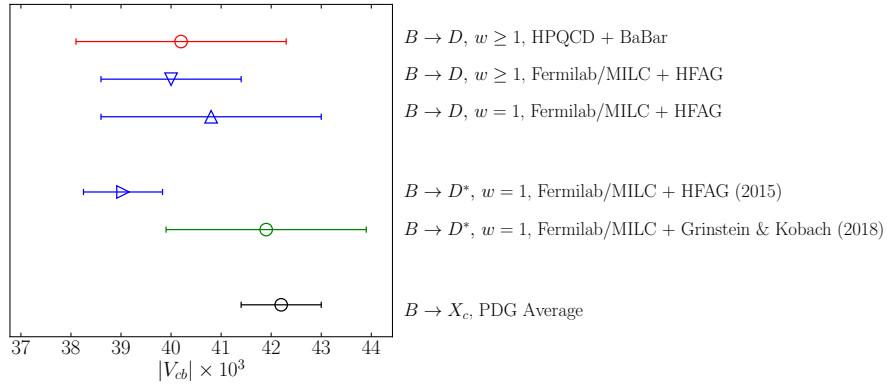


Figure 2.6: Different determinations of $|V_{cb}|$. Points labelled $w = 1$ are determinations from extrapolating measurements of decay rates to the zero recoil point, and combined with a lattice determination of the form factor at zero recoil. Points labelled $w \geq 1$ are results from using a combination of both branching fractions and lattice form factors through some range of w . The first name mentioned in the labels give the source of the lattice form factors, and the second gives the source of the experimental data (e.g. the HPQCD+BaBar point used form factors from the HPQCD collaboration and data from the BaBar experiment. The highest point is from [5], the second and third highest from [6], fourth from [7], fifth from [8]. The bottom point is from the PDG [1], using data from the ALPEPH [9], Belle [10], BaBar [11,12], and CLEO [13] experiments.

there was a 3σ tension between determinations from the $B \rightarrow D^* l \nu$ decay, and inclusive decays. This was on its way to being resolved when concern was raised about the method of extrapolating experimental data for $B \rightarrow D^* l \bar{\nu}$ decay rates to the zero recoil point ($w = 1$).

The Heavy Flavour Averaging Group HFAG (Now HFLAV) determination of $|\eta_{\text{EW}} V_{cb} h_{A_1}(1)|$ in 2015 parameterised the form factors in the extrapolation using the CLN parameterisation (defined in section 3.3.2). It has become clear that the constraints the CLN parameterisation imposes on the form factors are not justified. In [8, 14], the results of an extrapolation using the CLN parameterisation were compared to results from a more general, model independent parameterisation, the BGL parameterisation. It was found that they differed by 3.5σ . Since the BGL makes less assumptions, one may consider this the more reliable result.

The $|V_{cb}|$ result using BGL to extrapolate the decay rates is given in the green point on fig. 2.6. Hence, if this work is to be trusted, the long-standing $|V_{cb}|$ tension has been resolved.

There are however a number of other reasons to be interested in studying $|V_{cb}|$, namely improving its precision. It is currently the least precisely determined element of the CKM matrix. It constrains one side of the unitarity triangle via the ratio $|V_{ub}|/|V_{cb}|$, so it is the bottleneck for precise tests of CKM unitarity. It is also a dominant uncertainty in the determination of the CP -violation parameter ϵ_K (that is currently at tension between the SM and experiment, see for example [?] where a 4σ tension is reported).

A dominant motivation for the work presented in this thesis is the quest for a more precise determination of $|V_{cb}|$. The main results are form factors for $B_s \rightarrow D_s l \bar{\nu}$ and $B_s \rightarrow D_s^* l \bar{\nu}$. The benefit of these determinations are two-fold. Firstly, they can be combined with future experimental measurements of $B_s \rightarrow D_s^{(*)} l \bar{\nu}$ decays for a new $|V_{cb}|$ determination. Increasing the number of independent determinations of $|V_{cb}|$ makes each result more robust. Secondly, they demonstrate that our approach in the lattice calculations work well and can therefore be applied to $B \rightarrow D l \bar{\nu}$ and $B \rightarrow D l \bar{\nu}$ form factors in the future.

2.2.4 Flavour Anomalies

The SM can be tested from studying semileptonic decays more directly, without any consideration of CKM elements. CKM-independent observables can be constructed by taking ratios of branching fractions for decays with common CKM dependence.

Then, form factors from lattice QCD can be used to form pure SM predictions of these ratios, and compared to purely experimental measurements of those ratios. Such comparisons have uncovered a number of tensions between the SM and experiment.

The ratios are defined by

$$R(X) = \frac{\mathcal{B}(B_q \rightarrow X_q \tau \nu_\tau)}{\frac{1}{2} [\mathcal{B}(B_q \rightarrow X_q e \nu_e) + \mathcal{B}(B_q \rightarrow X_q \mu \nu_\mu)]} \quad (2.37)$$

where X_q is any meson with valence quark content $x\bar{q}$. Branching fractions $\mathcal{B}(\alpha \rightarrow \beta)$ are equal to $\Gamma(\alpha \rightarrow \beta)/\Gamma(\alpha \rightarrow \{\gamma_i\})$ where γ_i are all possible final states. The numerator and denominator will have the same power of $|V_{bx}|$, so cancel in the ratio.

$R(D^*)$ contains a 2.1σ discrepancy [15]:

$$R(D^*)|_{\text{SM}} = 0.252(3) , R(D^*)|_{\text{LHCb}} = 0.336(27)_{\text{sys}}(30)_{\text{stat}} \quad (2.38)$$

The issue is similarly present for $R(D)$ [16]:

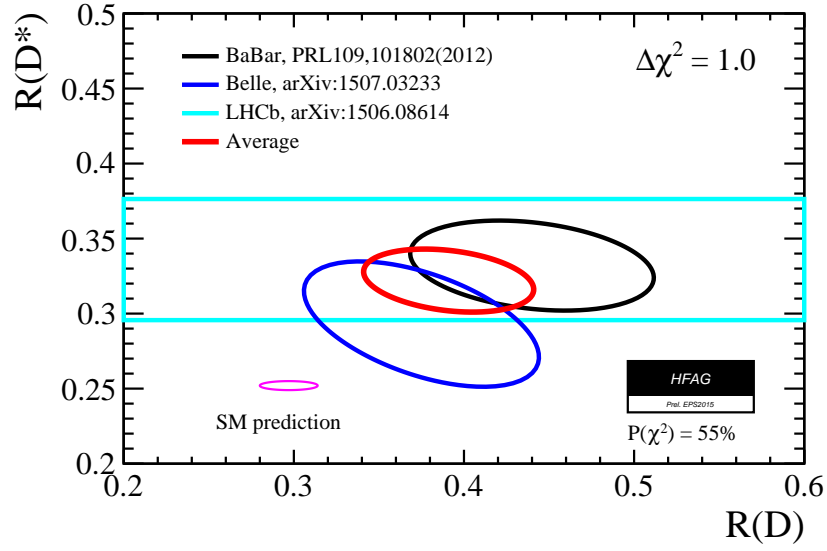
$$R(D)|_{\text{SM}} = 0.299(7) , R(D)|_{\text{exp}} = 0.391(28)_{\text{sys}}(41)_{\text{stat}} \quad (2.39)$$

where in this case $R(D)|_{\text{exp}}$ is a world average of experimental values. Our eventual study of $B \rightarrow D l \nu$ will produce a new standard model determination of $R(D)$, helping shed light on the issue.

Besides these, there are also tensions in the quantities [17]:

$$R'(K^{(*)}) = \frac{\mathcal{B}(B \rightarrow K^{(*)} \mu^+ \mu^-)}{\mathcal{B}(B \rightarrow K^{(*)} e^+ e^-)} \quad (2.40)$$

All of the above anomalies are suggestive of lepton flavour violating effects. Various BSM models have been suggested; hot topics include Leptoquarks, Z' models, and partial compositeness [17].

Figure 2.7: $R(D)/R(D^*)$ determinations from standard model and experiment [?]

Heavy \rightarrow Heavy Meson Semileptonic Decays

In this chapter we will review the key physical principles and theoretical machinery one needs to understand semileptonic decays involving heavy quarks. The presence of hadrons in these processes necessitates an introduction to strong interaction physics. The presence of heavy quarks offers us extra theoretical leverage to divide and conquer the different relevant scales of the decays.

3.1 Strong Interaction Physics

It has been pretty much established that the strong interaction, and the observed pattern of hadrons, can be explained with a non-abelian Yang-Mills field and a number of flavours of fermions (quarks) that interact with it [SO MUCH EVIDENCE]. In this section we review the main features of the fundamental theory, along with a useful effective theory for describing dynamics at the hadron level.

3.1.1 Quantum Chromodynamics

qcd lagrangian, symmetries, asymptotic freedom

Quantum Chromodynamics (QCD) is defined to be the $SU(3)$ Yang-Mills gauge theory. The Lagrangian is derived by requiring:

- N_f fermion fields transforming in the fundamental representation of an $SU(3)$ gauge group.
- Invariance under that gauge group.
- Renormalizability of all interactions.

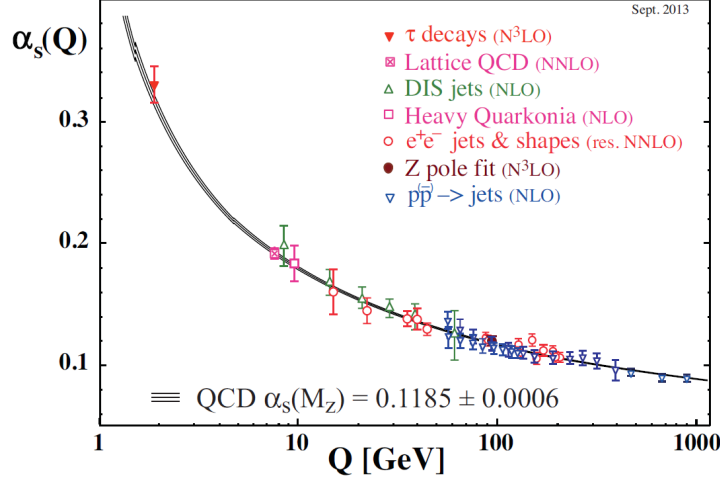


Figure 3.1: The relationship between scale Q and the strong coupling constant α_s , from the Particle Data Group [?]

From these we find [18]

$$\mathcal{L}_{\text{QCD}} = \sum_f \bar{q}_f (i\not{D} - m_f) q_f - \frac{1}{4} \text{Tr} G_{\mu\nu} G^{\mu\nu} - g \frac{\bar{\theta}}{64\pi^2} \epsilon^{\mu\nu\rho\sigma} \text{Tr} G_{\mu\nu} G_{\rho\sigma} \quad (3.1)$$

$$D_\mu = \partial_\mu - igG_\mu \quad (3.2)$$

$$G_{\mu\nu} = [D_\mu, D_\nu] \quad (3.3)$$

$q_f = (q_{f,r}, q_{f,b}, q_{f,g})$ are the N_f fermions, transforming under $q_f(x) \rightarrow U(x)q_f(x)$, $\bar{q}_f(x) \rightarrow \bar{q}_f(x)U^\dagger(x)$ where $U(x)$ is an $SU(3)$ matrix. G_μ are the $\mathfrak{su}(3)$ -valued gluon fields, transforming under $G_\mu(x) \rightarrow U(x)G_\mu(x)U^\dagger(x) - i/g[\partial_\mu U(x)]U^\dagger(x)$. g is the coupling constant of the theory, often expressed instead as $\alpha_s = (g/4\pi)^2$. $\bar{\theta}$ has strong experimental bounds on its size, to the extent for our purposes it can be neglected [19].

The most notable feature of QCD is due to the running of the QCD coupling α_s [20]. In contrast with the electroweak force, the coupling of the strong force diverges at low energies. This is referred to as *asymptotic freedom*. At energies at and below $\Lambda_{\text{QCD}} \sim 0.3\text{GeV}$, α_s becomes too large to be a good expansion parameter, and perturbation theory becomes unreliable for making predictions.

At large α_s , quarks and gluons become strongly interacting, this is believed

to be the source of confinement, the mechanism that bounds quarks together into hadrons. A common assumption then is that all of the dynamics that occurs inside hadrons have energies on the scale of Λ_{QCD} .

We arrive at the conclusion that processes involving hadrons cannot be understood using the traditional method of perturbation theory. Broadly speaking there are two alternative approaches:

1. Chiral Perturbation theory - an effective theory of hadrons with the same symmetry properties as QCD. This will be introduced in the next section.
2. Lattice simulations - solve the path integral by brute force, eliminating the need for an expansion in α_s . This is covered in sections 4 and 5, since it is the method used in the work presented in this thesis.

3.1.2 Chiral Symmetry

chiral symmetry, spontaneous SB,
explicit SB
WARD IDENTITIES
chiral pert. theory, pion octet.

In the limit of $m_f \rightarrow 0, \forall f$, QCD develops two new global symmetries between the flavours;

$$q_f(x) \rightarrow \exp(i\theta_a \lambda_a^{ff'}) q_{f'}(x) \quad (3.4)$$

$$q_f(x) \rightarrow \exp(i\gamma_5 \theta_a \lambda_a^{ff'}) q_{f'}(x) \quad (3.5)$$

where λ_a are $U(N_f)$ matrices. They are labelled $U(N_f)_V$ and $U(N_f)_A$ respectively, standing for vector and axial. Each of these groups can be decomposed into $U(1)_{V/A} \times SU(N_f)_{V/A}$, the $U(1)$ contains the single element corresponding to $\lambda_a = 1$, and $SU(N_f)$ contains the elements where λ_a are $SU(N_f)$ generators. Necessary? In the below we will take $N_f = 3$ when discussing physical aspects of the symmetry, since in the regime where chiral symmetry is important, the heavier three quarks do not effect the dynamics.

Via Noether's theorem, these symmetries imply currents that are conserved

in the massless limit [21];

$$V_\mu^a = \bar{q}\gamma_\mu\lambda_a q \quad , \quad \partial^\mu V_\mu^a = i\bar{q}[M, \lambda_a]q \quad (3.6)$$

$$A_\mu^a = \bar{q}\gamma_\mu\gamma_5\lambda_a q \quad , \quad \partial^\mu A_\mu^a = i\bar{q}\{M, \lambda_a\}\gamma_5 q \quad (3.7)$$

where $M = \text{diag}(m_u, m_d, m_s, \dots)$ acts on flavour. Since one can connect any two flavours via the $U(N_f)$ generators, one can build such currents charged with any combination of flavours from linear combinations of (3.6),(3.7), i.e.

$$V_\mu^{ff'} = \bar{q}_f\gamma_\mu q_{f'} \quad , \quad \partial^\mu V_\mu^{ff'} = i(m_f - m_{f'})S_{ff'} \quad (3.8)$$

$$A_\mu^{ff'} = \bar{q}_f\gamma_\mu\gamma_5 q_{f'} \quad , \quad \partial^\mu A_\mu^{ff'} = i(m_f + m_{f'})P_{ff'} \quad (3.9)$$

where $S_{ff'} = \bar{q}_f q_{f'}$, $P_{ff'} = \bar{q}_f \gamma_5 q_{f'}$ are the scalar and pseudoscalar densities. The non-conservation equations in (3.8),(3.9) are examples of Ward identities.

A useful theorem [22] is that partially conserved currents (currents that become conserved when some parameter in the theory vanishes, like $V_\mu^{ff'}$ and $A_\mu^{ff'}$) require no renormalization. This comes in useful when matching operators between regularization schemes, and will be used in [chapter N](#).

Spontaneous Chiral Symmetry Breaking

Besides the explicit breaking of chiral symmetry by the quark masses, the $U(N_f)_A$ symmetry is also *spontaneously broken* by the QCD dynamics. This is to say that, while the Lagrangian still holds this symmetry, the ground state of the theory is not invariant under such transformations;

$$Q_A^a|0\rangle \neq 0 \quad (3.10)$$

where $Q_A^a = \int d^3x A_0^a(x)$ is the conserved charge associated with the axial symmetry, and therefore also the generator of that symmetry acting on the Hilbert space [21].

There are three pieces of evidence for this claim.

- Scalar quark condensate. Using the comutation relations of $U(N_f)_A$, and assuming $Q_V^a|0\rangle = 0$, one can show that (3.10) implies

$$\langle 0|\bar{u}u|0\rangle = \langle 0|\bar{d}d|0\rangle = \langle 0|\bar{s}s|0\rangle \neq 0 \quad (3.11)$$

This value has been calculated in [23] to be $\sim 290\text{GeV}$.

- Lack of Parity Doubling. Q_A^a transforms states to states with opposite parity. If Q_A^a was unbroken we could say that $[Q_A^a, H] = 0$ (H is the Hamiltonian), and from this demonstrate a degeneracy between states of opposite parity that interact with the strong force, for example a degeneracy between scalar and pseudoscalar particles. However, Pseudoscalar particles are not even approximately degenerate to scalar particles [?].
- The Light Pseudoscalar Octet. Goldstone's theorem says that for every spontaneously broken generator, there should be a massless spin-zero excitation with the same quantum numbers as that generator (Goldstone boson). In the case of $N_f = 3$, 8 the broken Q_A^a 's would lead to an octet of massless pseudoscalar particles. In the presence of explicit symmetry breaking by the quark masses, these pseudoscalars would not be massless but have small masses proportional to the quark masses (pseudo-Goldstone bosons). This is exactly what is observed: there is an octet of pions, kaons and η particles that have masses ($\sim 200\text{MeV}$) much lower than any other states in QCD (e.g. the ρ meson, with mass $\sim 1\text{GeV}$) [ref!](#).

Chiral Perturbation Theory (χPT)

Chiral Perturbation Theory is an effective theory of the pseudo-Goldstone bosons in the massless limit. It is useful for lattice calculations as it gives us information about how observables in strongly interacting systems should vary with light quark mass. This can be used when extrapolations in light quark masses are performed. It is also a useful language for understanding finite volume effects in lattice simulations, since a finite volume will effect the lightest degrees of freedom in the system.

Terms in χPT are organized by number of derivatives acting on the fields, since we assume the excitations to have small masses (proportional to light quark masses), and are approximately on-shell.

Goldstone's theorem tells us that the (pseudo-)Goldstone bosons should have the same transformation properties under the chiral symmetry as the broken generators, in our case those of $SU(3)_A$. Using this, and the requirement that the theory should be $SU(3)_V$ invariant, we can write down the leading order

Lagrangian (minimal number of derivatives):

$$\mathcal{L}_2 = \frac{f^2}{4} \text{Tr}[\partial_\mu U \partial^\mu U^\dagger] \quad (3.12)$$

$$U = \exp\left(\frac{i}{f} \sum_{a=1}^8 \lambda_a \phi_a\right) \quad (3.13)$$

λ_a are $SU(3)$ generators and ϕ_a are the eight Goldstone bosons.

Connections between χ PT and QCD can be found by considering how external fields interact with either of the theories. For example, one can consider the quark masses in QCD as external scalar fields which couple to scalar currents $\bar{q}_f q_f$ and obtain a vev. One then asks: how would this field have to transform under the chiral symmetry for QCD to be $SU(3)_V$ invariant? So we are imagining $M = \text{diag}(m_u, m_d, m_s, \dots)$ is a field that transforms like

$$M \rightarrow \exp(i(1 - \gamma_5)\theta_a \lambda_a) M \exp(-i(1 + \gamma_5)\theta_b \lambda_b) \quad (3.14)$$

One then transitions into χ PT and asks: what interactions between the Goldstone fields and M are allowed by $SU(3)_V$? The answer is

$$\mathcal{L}_M = \frac{f^2 B_0}{2} \text{Tr}[MU^\dagger + UM^\dagger] \quad (3.15)$$

where B_0 is a new parameter of the theory. By comparing ground state energies of the two theories, i.e. $\langle 0 | H_{\text{QCD}} | 0 \rangle = \langle 0 | H_{\chi\text{PT}} | 0 \rangle$, one can identify $B_0 = \langle \bar{u}u \rangle / f^2$. By expanding \mathcal{L}_M in powers of quark masses and $1/f$, one can find mass terms for the Goldstones. Three of the goldstones are mass eigenstates, with masses given by

$$M_{\pi^0}^2 = B_0(m_u + m_d) \quad (3.16)$$

$$M_{K^0}^2 = B_0 \left(\frac{1}{2}m_u + \frac{1}{2}m_d + m_s \right) \quad (3.17)$$

$$M_\eta^2 = \frac{2}{3}B_0 \left(\frac{1}{2}m_u + \frac{1}{2}m_d + 2m_s \right) \quad (3.18)$$

where π, K , and η correspond to the physical mesons π, K, η , since their masses approximately respect these relations. Other terms that come out of expanding \mathcal{L}_M become mixing terms between the ϕ_a 's, via these we can identify the rest of the fields with physical mesons, resulting in

$$\begin{aligned} \pi^0 &= \phi_3 & K^0/\bar{K}^0 &= (\phi_6 \pm i\phi_7)/\sqrt{2} & \eta &= \phi_8 \\ \pi^\pm &= (\phi_1 \pm i\phi_2)/\sqrt{2} & K^\pm &= (\phi_4 \pm i\phi_5)/\sqrt{2} \end{aligned} \quad (3.19)$$

By a similar process one can deduce the Chiral currents in χ PT, for example the axial current is given by $A_\mu^a = if^2 \text{Tr}[\lambda_a(U^\dagger \partial_\mu U - (\partial_\mu U)U^\dagger)]/4$. By computing $\langle 0|A_\mu^3|\pi^0\rangle = M_{\pi^0}f_{\pi^0}$, one can identify the parameter f to be equal to the Pion decay constant f_{π^0} at leading order in χ PT.

Predictions in χ PT can be systematically improved by including terms with more derivatives in $\mathcal{L}_{\chi\text{PT}}$.

3.2 Heavy Quark Physics

Quarks with mass $m_Q \gg \Lambda_{\text{QCD}}$ are referred to as heavy quarks. Charm and bottom quarks are considered heavy: $\Lambda_{\text{QCD}}/m_c \sim 1/4$, $\Lambda_{\text{QCD}}/m_b \sim 1/14$. This separation of scales can come in very useful. They mean one can integrate out the degrees of freedom at m_Q , and still have a good description of the dynamics at Λ_{QCD} . As will be demonstrated, this does not mean totally removing the heavy quark from the theory.

The physical picture of a meson containing a heavy quark is very similar to that of a hydrogen atom. In the hydrogen atom, the nucleus has a mass much greater than the characteristic energies of the electron and photons. One can treat the nucleus as a static source of electric charge, and solve to high precision the dynamics of the electron. The electron's behaviour is not affected by the mass or the spin of the nucleus. Similarly, one can consider a heavy quark in a meson to be a static source of color charge, and solve the Λ_{QCD} dynamics in it's presence. The mass and spin of the heavy quark does not effect the light degrees of freedom, this is the well understood *heavy quark symmetries*. The effective field theories introduced in this section gives us a framework to take this approximation and systematically correct for it.

3.2.1 HQET

derivation of leading order HQET

form factors in HQET, isgur-wise function

luke's theorem

Heavy Quark Effective Theory (HQET) is an effective field theory with the cutoff at the heavy quark mass m_Q , and terms organized in a series in Λ_{QCD}/m_Q .

Since at the b (and c) mass QCD is perturbative ($\alpha_s(m_Q) \ll 1$), one can match HQET to perturbative QCD at m_Q , then run the couplings of HQET down to produce useful predictions at the confinement scale.

It is a useful tool for when we perform extrapolations in heavy quark mass, as it supplies us with explicit expressions for the heavy quark mass dependance on various phenomenological quantities.

HQET Lagrangian

As a simple example, we will derive HQET for a single heavy quark interacting with gluons. The fermion part of the Lagrangian is

$$\mathcal{L}_{\text{QCD}} = \bar{Q}(i\not{D} - m_Q)Q, \quad (3.20)$$

where Q is the heavy quark field. Define the heavy quark velocity v according to

$$v = \frac{p_Q}{m_Q}. \quad (3.21)$$

Now split Q into "heavy" and "light" components:

$$Q = h + H \quad : \quad h = \frac{1}{2}e^{-im_Q v \cdot x}(1 + \not{v})Q \quad (3.22)$$

$$H = \frac{1}{2}e^{-im_Q v \cdot x}(1 - \not{v})Q \quad (3.23)$$

with the important property

$$\not{v}h = h \quad \not{v}H = -H. \quad (3.24)$$

In terms of these new fields the Lagrangian becomes

$$\mathcal{L}_{\text{QCD}} = i\bar{h}(v \cdot D)h - \bar{H}(i(v \cdot D) - 2m_Q)H + i\bar{h}\not{D}^\perp H + i\bar{H}\not{D}^\perp h. \quad (3.25)$$

where $v_\mu(v \cdot D)$ is the covariant derivative projected along the direction of v , and $D^\perp = D - v_\mu(v \cdot D)$ is the components perpendicular to v . In the rest frame of the heavy quark, $v = (1, 0, 0, 0)$ so $v_\mu(v \cdot D)$ becomes the temporal derivative and D^\perp the spacial. The physical interpretation of the above definition can be seen by acting a spacial derivative on the definition of h , and by recognising $\partial Q = -ip_Q$, $\partial h = -ip_h$, we find that

$$p_Q = m_Q v + p_h \quad (3.26)$$

Since $p_h \ll p_Q$, we see that the quark's momentum is dominated by its mass (the quark is close to on-shell), and the h field represents perturbations around on-shell due to interactions with the lighter degrees of freedom at Λ_{QCD} .

From (3.25), we see that h is a massless field and H has a mass of $2m_Q$. From this Lagrangian we can derive an equation of motion for H :

$$(i(v \cdot D) + 2m_Q)H = i\not{D}^\perp h, \quad (3.27)$$

with the solution

$$H = \frac{1}{i(v \cdot D) + 2m_Q} i\not{D}^\perp h = \frac{1}{2m_Q} \sum_{n=0}^{\infty} \frac{(-i(v \cdot D))^n}{2m_Q} \not{D}^\perp h. \quad (3.28)$$

By substituting this into the Lagrangian we arrive at

$$\mathcal{L}_{\text{HQET}} = i\bar{h}(v \cdot D)h - \bar{h}\not{D}^\perp \frac{1}{2m_Q} \sum_{n=0}^{\infty} \frac{(-i(v \cdot D))^n}{2m_Q} \not{D}^\perp h. \quad (3.29)$$

This can be found by a more rigorous proof by performing the Gaussian integration over the H field in the path integral [ref!](#). Since we expect $v \cdot D \sim \Lambda_{\text{QCD}}$, we can interpret the infinite sum as a series in Λ_{QCD}/m_Q , and truncate it at some order. For example to $\mathcal{O}(\Lambda_{\text{QCD}}/m_Q)$, we have

$$\mathcal{L}_{\text{HQET}^1} = i\bar{h}(v \cdot D)h - \frac{1}{2m_Q} \bar{h}\not{D}^{\perp 2}h \quad (3.30)$$

Leading order HQET exhibits new symmetries not present in full QCD, known as the heavy quark symmetries. Since m_Q is not present in the leading order Lagrangian, there is a flavour symmetry - a set of N heavy quarks with the same v can be mixed via an $SU(N)$ symmetry. Similarly due to the absence of spin mixing matrices, a heavy quark has an $SU(2)$ spin symmetry. This builds up a physical picture of a heavy quark in a meson being a static colour charge, the dynamics at Λ_{QCD} is not effected by its mass or spin.

Isgur-Wise Function

A consequence of heavy quark symmetry relevant to semileptonic decays are the Wigner-Eckart theorems. Consider a transition amplitude between two heavy pseudoscalar mesons:

$$\langle M(v) | \bar{h} \Gamma h | M(v') \rangle \quad (3.31)$$

The spin structure of $|M(v)\rangle$ is $\gamma_5(1-\not{v})$, this can be shown with the following argument. The state can be generally written as $|M(v)\rangle = \int d^4x d^4y f(x, y) \bar{h}(x) \gamma_5 q(y) |\Omega\rangle$ which, using $\not{v}h = h$, can be reexpressed as $|M(v)\rangle = \int d^4x d^4y f(x, y) \bar{h}(x) \gamma_5(1 - \not{v})q(y) |\Omega\rangle/2$. Then via the spin symmetry, one can always rotate the h spin in the meson state such that it matches the spin of the current, i.e. $h_\alpha \bar{h}_\beta \rightarrow 1_{\alpha\beta} f(h, \bar{h})$. Then the amplitude can be written as

$$\langle M(v) | \bar{h} \Gamma h | M(v') \rangle = m_M \text{Tr} \left[\frac{1}{2} \gamma_5 (1 - \not{v}) \Gamma \frac{1}{2} \gamma_5 (1 - \not{v}') \mathcal{M}(v, v') \right] \quad (3.32)$$

where $\mathcal{M}(v, v')$ can be any gamma-matrix valued function. The m_M factor comes from the relativistic normalization of the states. A general spin decomposition of this is

$$\mathcal{M}(v, v') = \xi_0(v \cdot v') + \not{v} \xi_1(v \cdot v') + \not{v}' \xi_2(v \cdot v') + \not{v} \not{v}' \xi_4(v \cdot v'). \quad (3.33)$$

Plugging this into (3.32), we can then write the amplitude in terms of a single function:

$$\langle M(v) | \bar{h} \Gamma h | M(v') \rangle = m_M \text{Tr} \left[\frac{1}{2} \gamma_5 (1 - \not{v}) \Gamma \frac{1}{2} \gamma_5 (1 - \not{v}') \right] \xi(v \cdot v') \quad (3.34)$$

where $\xi(v \cdot v') = \xi_0(v \cdot v') + \xi_1(v \cdot v') - \xi_3(v \cdot v') - \xi_4(v \cdot v')$ is known as the Isgur-Wise function. For a general pair of mesons with spin structure $\mathcal{H}, \mathcal{H}'$, a transition amplitude between them with a heavy current insertion can always be written as

$$\langle \mathcal{H} | \bar{h} \Gamma h | \mathcal{H}' \rangle = \xi(v \cdot v') \text{Tr} [\bar{\mathcal{H}} \Gamma \mathcal{H}] + \mathcal{O} \left(\frac{\Lambda_{\text{QCD}}}{m_Q} \right) \quad (3.35)$$

So all heavy semileptonic decays involving any combination of masses or spins are described by a single non-perturbative function, $\xi(v \cdot v')$. A couple of relevant examples are:

$$\langle D(v') | \bar{c}_{v'} \gamma^\mu b_v | \bar{B}(v) \rangle = \sqrt{m_B m_D} (v + v')^\mu \xi(v \cdot v') \quad (3.36)$$

$$\langle D^*(v') | \bar{c}_{v'} \gamma^\mu b_v | \bar{B}(v) \rangle = i \sqrt{m_B m_D} \epsilon^{\mu\nu\alpha\beta} \varepsilon_{\nu}^* v'_\alpha v_\beta \xi(v \cdot v') \quad (3.37)$$

$$\langle D^*(v') | \bar{c}_{v'} \gamma^\mu \gamma_5 b_v | \bar{B}(v) \rangle = \sqrt{m_B m_D} [\varepsilon^{*\mu} (v \cdot v' + 1) - v'^\mu \varepsilon^* \cdot v] \xi(v \cdot v'). \quad (3.38)$$

Here we have subscripted the fields $c_{v'}, b_v$ to specify the velocity used to separate those fields from the heavy components e.g. in eq. (3.22).

AG and Luke's Theorem

Luke's theorem, which can be derived from the Ademollo-Gatto (AG) theorem, tells us the leading order heavy quark mass dependence of form factors. First we

will derive the AG theorem. We will follow the proof given in [24].

Consider the transition amplitude

$$\langle \alpha | Q_a | \beta \rangle \quad (3.39)$$

where Q_a is a conserved charge associated with some global symmetry \mathcal{G} , and $|\alpha\rangle$ and $|\beta\rangle$ belong to an irrep of \mathcal{G} . Imagine explicitly breaking the symmetry with a term like $\mathcal{L}_{\text{break}} = \lambda \mathcal{O}_{\text{break}}$. The states in the broken theory can be expressed as

$$|\beta\rangle = c_{\beta\beta} |\beta'\rangle + \sum_m c_{\beta m} |m'\rangle \quad (3.40)$$

$$\langle \alpha | = c_{\alpha\alpha}^* \langle \alpha' | + \sum_n c_{\alpha n}^* \langle n' |. \quad (3.41)$$

where primed states are states belonging to irreps of \mathcal{G} . Here $|m'\rangle$ can only be states that can be mixed with $|\beta\rangle$ by $\mathcal{O}_{\text{break}}$ via the broken dynamics of the theory, and similarly for $\langle n' |$ and $\langle \alpha' |$. The transition amplitude becomes

$$\begin{aligned} \langle \alpha | Q_a | \beta \rangle &= c_{\alpha\alpha}^* c_{\beta\beta} \langle \alpha' | Q_a | \beta' \rangle \\ &+ \sum_m c_{\alpha\alpha}^* c_{\beta m} \langle \alpha' | Q_a | m' \rangle \\ &+ \sum_n c_{\alpha n}^* c_{\beta\beta} \langle n' | Q_a | \beta \rangle \\ &+ \sum_m \sum_n c_{\alpha n}^* c_{\beta m} \langle n' | Q_a | m' \rangle \end{aligned} \quad (3.42)$$

The theorem applies to the situation where $|n'\rangle$ and $|m'\rangle$ live in different \mathcal{G} irreps to $|\alpha\rangle$ and $|\beta\rangle$ (we assume $|\alpha\rangle$ and $|\beta\rangle$ to be in the same irrep otherwise the transition amplitude will always be zero). In this case the amplitudes in the second and third terms vanish. Now consider the order of the coefficients c_{nm} . We can assume that $c_{nm} = \mathcal{O}(\lambda)$ for arbitrary $n, m \neq \alpha, \beta$, since switching off the symmetry breaking by setting $\lambda = 0$ should cause $|\alpha\rangle$ and $|\alpha'\rangle$ to coincide. Then, using the normalization of the states $\sum_n |c_{\alpha n}|^2 = 1$, we find $c_{\alpha\alpha} = \sqrt{1 - \mathcal{O}(\lambda)^2} = 1 + \mathcal{O}(\lambda^2)$, and similarly for $c_{\beta\beta}$. Applying this to the two surviving terms in (3.42), we end up with

$$\langle \alpha | Q_a | \beta \rangle = 1 + \mathcal{O}(\lambda^2) \quad (3.43)$$

This is the AG theorem: if the current Q_a and the symmetry breaking term \mathcal{O} act orthogonally on the states, the transition amplitude can have at most a second order correction in the symmetry breaking parameter.

Now we will apply this to HQET to produce Luke's theorem. Consider a transition including two heavy quarks (b and c). Then, the heavy quark symmetry is a spin symmetry for each flavour, and a flavour symmetry between them. The leading order spin symmetry breaking terms can be found from (3.30) to be

$$\frac{1}{4m_Q} \bar{h} \gamma^\mu \gamma^\nu F_{\mu\nu} h \quad (3.44)$$

for both $h = b$ and $h = c$. The leading order flavour breaking term is

$$\left(\frac{1}{2m_b} - \frac{1}{2m_c} \right) \frac{1}{2} \bar{h} \sigma_z \not{D}^{\perp 2} h \quad (3.45)$$

where now $h = (b, c)$ and the σ_z is the third pauli matrix acting on flavour. These terms cause states, for example $|B\rangle$ to mix with states $|n'\rangle$, each being of the order of at least one of the following: $1/2m_b, 1/2m_c$, and $(1/2m_b - 1/2m_c)$. It can be shown ([24]) that the leading order symmetry breaking terms can only mix pseudoscalar and vector mesons with other irreps of the heavy quark symmetries. Hence, for example the example of the $B \rightarrow D$ transition, where

$$\langle D | \bar{c} \gamma_\mu b | B \rangle = 1 + \mathcal{O}(\epsilon_b^2) + \mathcal{O}(\epsilon_c^2) \quad (3.46)$$

$$+ \mathcal{O}((\epsilon_b - \epsilon_c)^2). \quad (3.47)$$

where we have now defined $\epsilon_h = 1/2m_h$. This implies the Isgur-Wise function ξ also has corrections of this order. As we move away from the infinite-mass limit, ξ becomes h_+ , and h_- becomes non-zero. In this case we see that

$$h_+(q_{\max}^2) = 1 + \mathcal{O}(\epsilon_b^2) + \mathcal{O}(\epsilon_c^2) \quad (3.48)$$

$$+ \mathcal{O}((\epsilon_b - \epsilon_c)^2) \quad (3.49)$$

$$h_-(q_{\max}^2) = \mathcal{O}(\epsilon_b) + \mathcal{O}(\epsilon_c) + \mathcal{O}(\epsilon_b - \epsilon_c) \quad (3.50)$$

Away from q_{\max}^2 , the velocities for the b and c quarks become different, resulting in a new flavour breaking term in the effective Lagrangian;

$$i\bar{c}(v - v') \cdot D c \sim \mathcal{O}\left(1 - \frac{E_D}{M_D}\right) + \mathcal{O}\left(\frac{p_D}{M_D}\right) \quad (3.51)$$

where to deduce the orders we took the rest frame of the B meson. This results in extra corrections of these orders (raised to the second power) in the form factors.

Second Order Form Factors

The process in 3.2.1 of decomposing matrix elements into general expressions parameterized by non-perturbative functions can be extended beyond leading order in HQET. In [25] this process was continued to second order in $1/m_b$ and $1/m_c$ for $B \rightarrow D^{(*)}$ transitions. The form factors for general v, v' that are relevant to our work, were found to have the forms

$$h_+ = \xi + (\epsilon_b + \epsilon_c)L_1 + (\epsilon_b^2 + \epsilon_c^2)l_1 + \epsilon_b\epsilon_c\phi_1 \quad (3.52)$$

$$h_- = (\epsilon_c - \epsilon_b)L_4 + (\epsilon_c^2 - \epsilon_b^2)l_4 \quad (3.53)$$

$$h_{A_1} = \xi + \epsilon_c L_{25} + \epsilon_b L_{14} + \epsilon_c^2 l_{25} + \epsilon_b^2 l_{14} + \epsilon_c \epsilon_b \phi_2 \quad (3.54)$$

where, due to the normalization of the form factors for $m_c = m_b$ at q_{\max}^2 ;

$$L_1(q_{\max}^2) = L_{25}(q_{\max}^2) = L_{14}(q_{\max}^2) = 0 \quad (3.55)$$

A calculation using the non-relativistic constituent quark model [?] estimates the factor $l_1(q_{\max}^2) = -3m_q^2$ where q is the spectator of the decay.

Decay Constants

questions that still need answered:

1) how come the $\sqrt{m_b}$ from state normalizations don't appear in h_+ etc? 2) how much does the above stuff apply away from continuum limit?

3.2.2 NRQCD

NRQCD motivation

'derivation' of NRQCD

foldy-wouthousiusen transform

An effective field theory closely related to HQET is Non-Relativistic QCD (NRQCD). This differs from HQET only by the power counting; instead of organizing terms in the Lagrangian according to their order in Λ_{QCD}/m , the terms are organized in terms of orders of the heavy quark's spacial velocity $v \sim p/m$ (where now $p = |\underline{p}|$). NRQCD is derived with the following process:

- Separate the quark and antiquark components of the heavy quark Q . Define the antiquark-free 2-component spinor h via $Q = e^{\gamma \cdot \nabla / 2m} \begin{pmatrix} h \\ 0 \end{pmatrix}$ [26].

- Define power-counting by considering the expected expectation values of operators for heavy mesons [27]. The three relevant scales concerning the heavy meson are $M, p \sim Mv$ and $E_K \sim Mv^2$, where M is the meson mass, p the spacial momentum and E_K the kinetic energy. By relating operators to these three scales, we deduce their order in v . Start with the normalization of a scalar current:

$$\langle M | \int d^3x h^\dagger(x) h(x) | M \rangle \sim 1 \quad (3.56)$$

where $|M\rangle$ is some heavy meson state. Since we expect the meson state to be localized in a region of size $1/p$, we can assert that

$$\int d^3x \sim \frac{1}{p^3} \quad (3.57)$$

from this and (3.56), we find $h \sim p^{3/2} \sim v^{3/2}$. The order of the derivative operator can be deduced from

$$E_K = \langle M | \int d^3x h^\dagger(x) \frac{D^2}{2M} h(x) | M \rangle \quad (3.58)$$

to be $D \sim v$. Following such a chain of arguments, we can deduce the order in v of any operator.

- The Lagrangian to $\mathcal{O}(v^n)$ is then simply all of the operators satisfying the symmetries of QCD of orders below v^n , with some Wilson coefficients [27]. To $\mathcal{O}(v^6)$:

$$\begin{aligned} \mathcal{L}_{\text{NRQCD}} = & h^\dagger \left(iD_0 + \frac{D^2}{2m} + c_1 \frac{D^4}{m^3} + c_2 g \frac{\underline{D} \cdot \underline{E} - \underline{E} \cdot \underline{D}}{m^2} \right. \\ & + c_3 i g \frac{\underline{\sigma} \cdot (\underline{D} \times \underline{E} - \underline{E} \times \underline{D})}{m^2} + c_4 g \frac{\underline{\sigma} \cdot \underline{B}}{m} \\ & \left. + f_1 g \frac{\{\underline{D}^2, \underline{\sigma} \cdot \underline{B}\}}{m^3} + f_2 i g \frac{\{\underline{D}^2, \underline{\sigma} \cdot (\underline{D} \times \underline{E} - \underline{E} \times \underline{D})\}}{m^4} + f_3 i g^2 \frac{\underline{\sigma} \cdot \underline{E} \times \underline{E}}{m^3} \right) h \\ & + d_1 \frac{(h^\dagger H)(H^\dagger h)}{m^2} + d_2 \frac{(h^\dagger \underline{\sigma} H) \cdot (H^\dagger \underline{\sigma} h)}{m^2} \\ & + d_3 \sum_a \frac{(h^\dagger T^a H)(H^\dagger T^a h)}{m^2} + d_4 \sum_a \frac{(h^\dagger T^a \underline{\sigma} H) \cdot (H^\dagger T^a \underline{\sigma} h)}{m^2} \end{aligned} \quad (3.59)$$

\underline{E} and \underline{B} are the chromoelectric and chromomagnetic fields, T^a are $SU(3)$ color generators, and H is the antiquark components of the heavy quark. The Wilson coefficients are fixed by perturbative matching to full QCD at the cutoff (the heavy quark mass, where QCD is perturbative), then the coefficients can be run down to the scale of interest.

3.3 Form Factors

define form factors in the pseudoscalar-pseudoscalar and pseudoscalar-vector cases. both 'experimental' and 'hqet' versions...

The goal of this work is to compute the transition amplitudes that make up the non-perturbative part of semileptonic decays, i.e. $H_\mu = \langle H_2 | J_\mu | H_1 \rangle$, where $H_{1,2}$ are initial and final meson states and J_μ is a current representing the emission of a W^\pm .

We will refer to the 4-momenta and mass of the initial and final states as $p_{1,2}, M_{1,2}$ respectively, and define the 4-momentum taken away by the W^\pm boson as $q \equiv p_2 - p_1$. We work in the rest frame of the initial meson, in which

$$q^2 = M_1^2 + M_2^2 - 2M_1 E_2. \quad (3.60)$$

There is a physically allowed range of values for an on-shell q^2 . The minimum is when all of the 3-momentum of the initial state is taken by the final meson, $q_{\min}^2 = 0$. q^2 is maximised when all of the 3-momentum is taken by the boson, $\underline{p}_2^2 = 0 \rightarrow E_2 = \sqrt{M_2^2 + \underline{p}_2^2} = M_2 \rightarrow q_{\max}^2 = M_1^2 - M_2^2 - 2M_1 M_2 = (M_2 - M_1)^2$. So

$$0 \leq q^2 \leq (M_2 - M_1)^2 \quad (3.61)$$

This also creates an allowed range for the final meson 3-momentum:

$$0 < \underline{p}_2^2 < \left(\frac{M_1^2 + M_2^2}{2M_1} \right)^2 - M_2^2 \quad (3.62)$$

To make the connection with experiment, H_μ must be expressed in terms of Lorentz-invariant factors, known as *form factors*. The current operator between between the states is a conserved current, so then the matrix element must be proportional to only conserved quantities, namely, elements of the stress-energy tensor. Lorentz invariance requires indices on either side of such a relation match, so a matrix element with a single Lorentz index can only be proportional to 4-momenta.

There are two cases of interest: the pseudoscalar \rightarrow pseudoscalar and pseudoscalar \rightarrow vector. Let us consider the first case first, with a the insertion of a left-handed current representing an emission of a W^\pm . From eq. (weak decays section), the coupling of quarks q_1 and q_2 to the W^\pm is given by $L_\mu = \bar{q}_2 \gamma_\mu \frac{1}{2}(1 - \gamma_5) q_1$.

This can be written as $L_\mu = V_\mu - A_\mu$, these are the vector and axial vector currents.

The axial vector evaluated between two pseudoscalar states must vanish because the combination is not parity invariant thus does not contribute in pure QCD, leaving just the vector current. The most common parameterisation used in the experiment community is:

$$\langle P_2(p_2) | V^\mu | P_1(p_1) \rangle = f_+(q^2) \left[p_1^\mu + p_2^\mu - \frac{M_1^2 - M_2^2}{q^2} q^\mu \right] + f_0(q^2) \frac{M_1^2 - M_2^2}{q^2} q^\mu \quad (3.63)$$

Where $|P_i(p_i)\rangle$ is a pseudoscalar meson state with momentum p_i .

3.3.1 Analyticity

analytic structure, branch cut, subthreshold poles etc.

$q^2 \rightarrow z$ mapping

3.3.2 Parameterisations

brief description of CLN, explain why it's garbage

BGL & BCL, explain why it's great

3.4 Experimental Status

list of things semileptonic decays that have been measured and their measurements,
decays that in principle will be measured in the future...

Lattice Quantum Chromodynamics

path integral

discretisation of path integral, summary of steps in a lattice calculation (like, a couple of sentences)

At low energies ($\sim 200\text{MeV}$ and below), QCD becomes non-perturbative, in other words, the coupling α_s becomes $\mathcal{O}(1)$, and an expansion in α_s (as in perturbation theory) will not be dominated by the leading orders [18]. We require an alternative.

The expectation value of an observable \mathcal{O} in a Yang-Mills theory can be expressed as a Euclidean path integral [28];

$$\langle \mathcal{O} \rangle = \int \mathcal{D}A \mathcal{D}\psi \mathcal{D}\bar{\psi} \mathcal{O} e^{-S[A, \psi, \bar{\psi}]}, \quad (4.1)$$

where A is a gauge field, $\psi(\bar{\psi})$ is an (anti)fermion field, S is the Euclideanised classical action, and \mathcal{D} denotes integration over all configurations of a field. "Euclideanised" refers to a Wick rotation $t \rightarrow it$ in S . In the perturbative approach, we would expand $\exp(-\text{interacting part of } S)$ resulting in a power series in the gauge coupling populated by Feynman diagrams.

The other option is to instead carry out the integral directly. This can only be done numerically. Since it's not numerically feasible to carry out an infinite number of integrals, one must approximate spacetime as a discrete 4 dimensional lattice with spacing " a " between lattice sites, finite spacial volume L_x^3 and finite temporal extent L_t . The functional integral becomes

$$\int \mathcal{D}A \mathcal{D}\psi \mathcal{D}\bar{\psi} = \prod_n \int dU(x_n) d\psi(x_n) d\bar{\psi}(x_n), \quad (4.2)$$

where n is a 4-vector with integer components labelling the sites, and $x_n^\mu = an^\mu$. This has a second benefit which is to naturally regularize the theory with a momentum

cutoff $\Lambda \sim 1/a$ [28]. The gauge field has been replaced with the gauge “link”:

$$U_\mu(x) \equiv \exp \left(i g a A_\mu \left(x + \frac{a\hat{\mu}}{2} \right) \right) \in SU(N_c), \quad (4.3)$$

g is the gauge coupling, $\hat{\mu}$ is a unit vector in the μ direction. Parameterizing the gauge fields this way is motivated by the geometrical interpretation of Yang-Mills theories on discrete spacetime and the requirement of exact gauge symmetry [29].

4.1 Lattice Gauge Fields

differential geometry in gauge theory, fibre bundles etc.

4.1.1 The Wilson Gauge Action

wilson action

4.1.2 Improvements

general idea of symanzik improvements

the gluon action used in milc code

4.2 Lattice Fermions

naive fermion discretisation

The interacting Dirac action is most naively discretised with

$$S_F = \sum_{x,\mu} \bar{\psi}(x) \gamma_\mu \nabla_\mu \psi(x) + m \sum_x \bar{\psi}(x) \psi(x), \quad (4.4)$$

where ∇_μ is the gauge covariant finite difference operator,

$$\nabla_\mu \psi(x) = \frac{1}{2a} (U_\mu(x) \psi(x + a\hat{\mu}) - U_\mu^\dagger(x - a\hat{\mu}) \psi(x - a\hat{\mu})). \quad (4.5)$$

In appendix ?? we describe the doubling problem. This is the observation that the propagator for a fermion obeying (4.7), $M^{-1}(k)$ has the property

$$M^{-1}(k + \frac{\pi}{a}\zeta) = \gamma_{5\mu} M^{-1}(k) \gamma_{5\mu} \quad (4.6)$$

For 16 4-vectors $\zeta_\mu \in \mathbb{Z}_2$. This leads to 16 poles in the fermion spectrum, therefore 16 distinct excitations (called *tastes*). We require a way of removing the 15 unphysical excitations.

4.2.1 The Doubling Problem

doubling symmetry \rightarrow 16 excitations

The interacting Dirac action is most naively discretised with

$$S_F = \sum_{x,\mu} \bar{\psi}(x) \gamma_\mu \nabla_\mu \psi(x) + m \sum_x \bar{\psi}(x) \psi(x), \quad (4.7)$$

where ∇_μ is the gauge covariant finite difference operator,

$$\nabla_\mu \psi(x) = \frac{1}{2a} (U_\mu(x) \psi(x + a\hat{\mu}) - U_\mu^\dagger(x - a\hat{\mu}) \psi(x - a\hat{\mu})). \quad (4.8)$$

An issue arises with fermions on the lattice, known as the doubling problem. S_F is invariant under a so-called "doubling symmetry", which is generated by

$$\psi(x) \rightarrow \mathcal{B}_\mu \psi(x) \equiv (-1)^{x_\mu/a} \gamma_{5\mu} \psi(x) \quad (4.9)$$

$$\bar{\psi}(x) \rightarrow \bar{\psi}(x) \mathcal{B}_\mu^\dagger \equiv (-1)^{x_\mu/a} \bar{\psi}(x) \gamma_{5\mu}^\dagger \quad (4.10)$$

where $\gamma_{5\mu} = i\gamma_\mu \gamma_5$. The product space of these form a group of 16 elements $\{\mathcal{B}_\zeta\}$, labeled by vectors ζ with $\zeta_\mu \in \mathbb{Z}_2$ (e.g. the element $\mathcal{B}_0 \mathcal{B}_1$ is labeled by $\zeta = (1, 1, 0, 0)$).

The physical significance of this symmetry can be seen when we study its effect on the action. First, notice that

$$\mathcal{B}_\mu \psi(x) = \gamma_{5\mu} \sum_k \tilde{\psi}(k) e^{i(k + \frac{\pi}{a}\hat{\mu}) \cdot x} \quad (4.11)$$

$$= \gamma_{5\mu} \sum_k \tilde{\psi}(k - \frac{\pi}{a}\hat{\mu}) e^{ik \cdot x} \quad (4.12)$$

where k is a set of discrete 4-momenta. The action in momentum space can be written as

$$S = \sum_k \bar{\tilde{\psi}}(k) M(k) \tilde{\psi}(k) \quad (4.13)$$

after the operation of \mathcal{B}_μ it becomes

$$S \rightarrow \sum_k \bar{\tilde{\psi}}(k) \gamma_{5\mu} M(k + \frac{\pi}{a}\hat{\mu}) \gamma_{5\mu} \tilde{\psi}(k) \quad (4.14)$$

Since we know S is invariant under this transformation, it must be true that $\gamma_{5\mu} M(k + \frac{\pi}{a}\hat{\mu}) \gamma_{5\mu} = M(k)$, and therefore

$$M^{-1}(k + \frac{\pi}{a}\hat{\mu}) = \gamma_{5\mu} M^{-1}(k) \gamma_{5\mu} \quad (4.15)$$

M^{-1} is the propagator for the fermion field, so 4.15 shows that the spectrum of the fermion is periodic, with a period of π/a . We expect a pole in $M^{-1}(k)$ where $k \sim m$, where m is the pole mass of the fermion, but there will now be a second pole at $m + \pi/a$. This will be around the natural cutoff imposed by the lattice $1/a$, and any higher poles like $m + 2\pi/a$ is far above the cutoff so will not contribute.

Generalizing this argument to all elements of the doubling symmetry, we see that

$$M^{-1}(k + \frac{\pi}{a}\zeta) = \gamma_{5\mu} M^{-1}(k) \gamma_{5\mu} \quad (4.16)$$

leading to 16 poles in the fermion spectrum, therefore 16 distinct excitations (called *tastes*).

We now show that there are only 4 tastes in the staggered quark formalism. One can isolate a single taste by a block-scaling procedure:

$$\psi^{(\zeta)}(x_B) = \sum_{\delta x_\mu \in \mathbb{Z}_2} \mathcal{B}_\zeta \psi(x_B + \delta x) \quad (4.17)$$

For example, for $\zeta = 0$, it would only contain the original non-doubler taste, since all other poles at $|k| \sim \pi/a$ have been integrated out. For $\zeta \neq 0$, the \mathcal{B}_ζ operator pushes the ζ doubler to where the $\zeta = 0$ taste originally was in k space, then the blocking procedure integrates out the rest. Now writing this isolated taste in terms of χ we arrive at:

$$\psi^{(\zeta)}(x_B) = \sum_{\delta x_\mu \in \mathbb{Z}_2} \Omega(\delta x) \mathcal{B}_\zeta(0) \chi(x + \delta x) \quad (4.18)$$

Recall we set $\chi(x) = (\chi_1(x), 0, 0, 0)$. The product $\Omega(\delta x) \mathcal{B}_\zeta(0)$ is simply a product of gamma matrices, so can only serve to "scramble" the elements of χ . Then, in the staggered formalism, all 16 tastes $\psi^{(\zeta)}$ amount to only 4 distinguishable fermions: $(\chi_1, 0, 0, 0)$, $(0, \chi_1, 0, 0)$, $(0, 0, \chi_1, 0)$, $(0, 0, 0, \chi_1)$ (with factors of (-1) and i).

4.2.2 Staggered Quarks

staggered transformation

proof that there are only 4 doublers now

spin-taste basis

There are a number of solutions to this problem. The most straightforward is to modify the action to push the mass of the unwanted tastes above the momentum cutoff, preventing it from effecting the dynamics ("Wilson fermions") ([30] ch.6.2). However, actions of this type explicitly break Chiral symmetry. Among other issues, this causes additive renormalization of the fermion mass, immensely complicating the renormalization procedure.

Another approach, known as *staggered quarks* ([30] ch.6.3), partially resolves the doubling issue while retaining chiral symmetry. This is the method we use in our study. Other notable approaches besides Wilson and staggered quarks include *domain wall* [31] and *overlap* [32] fermions.

The general idea of staggered fermions is the following. Redefine the fields according to

$$\psi(x) = \prod_{\mu} (\gamma_{\mu})^{x_{\mu}/a} \chi(x) \equiv \Omega(x) \chi(x) \quad (4.19)$$

In terms of the new spinor variables $\chi(x)$, the naive action (4.7) becomes

$$S_F = \bar{\chi}(x) [\alpha_{\mu}(x) \nabla_{\mu} + m] \chi(x) \quad (4.20)$$

where $\alpha_{\mu}(x) = (-1)^{\sum_{\nu < \mu} x_{\nu}/a}$. The action is now diagonal in spin, leading to 4 decoupled grassman variables with identical actions and identical coupling to the gauge field. As a result, χ propagators (on fixed gauge backgrounds) are spin diagonal:

$$M_{\chi}^{-1}(x, y)[U] = s(x, y)[U] \mathbf{1}_{\text{spin}} \quad (4.21)$$

One need only to include a single component of χ in a simulation (i.e. fix $\chi = (\chi_1, 0, 0, 0)$). Then they can compute $M_{\chi}^{-1}(x, y)[U]$ to obtain $s(x, y)$. Then, using the inverse of (4.19), $s(x, y)$ can be transformed to a propagator of the original spinors:

$$M_{\psi}^{-1}(x, y)[U] = s(x, y)[U] \Omega(x) \Omega^{\dagger}(y) \quad (4.22)$$

This is clearly computationally beneficial. But also, by shaving off the other spinor components, one reduces the number propagating degrees of freedom by a factor of 4. This cuts the number of tastes from 16 down to 4 (this is shown in appendix ??).

The remaining multiplicity is tacked in 3 steps:

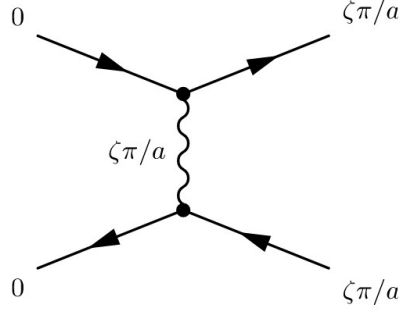


Figure 4.1: Taste mixing at tree level.

1. Ensure only one taste is created and destroyed in the propagator.
2. Minimize the interaction between tastes by modifying the action.
3. Remove contributions of extra tastes in the sea by taking $\det M \rightarrow \sqrt[4]{\det M}$ in (5.3).

Step 3 can be justified by the following - in the $a \rightarrow 0$ limit, $\det M$ tends to $(\det M^{(0)})^4$, where $M^{(0)}$ is the Dirac operator for a single taste. Then, taking the 4th root (in principle) reduces the determinant to that of a sea containing 1 taste.

4.2.3 Highly Improved Staggered Quarks

define HISQ

minimises taste exchange

removes some tree-level artifacts

Step 2 above is the guiding principle for the action we use in our study, the Highly Improved Staggered Quark action (HISQ).

Interaction between different tastes ("taste mixing") is dominated by the process in fig. 4.1. In HISQ, this is suppressed by modifying the gauge fields in such a way as to minimize the coupling between a gluon with momentum π/a and the fermions, in other words, minimize the vertices in fig. 4.1. To this end, one can change the action so that fermions only couple to *smeared* gauge links, in which high frequency excitations have been removed.

Define the first and second covariant derivative operators:

$$\begin{aligned}\delta_\rho U_\mu(x) &\equiv \frac{1}{a} (U_\rho(x) U_\mu(x + a\hat{\rho}) U_\rho^\dagger(x + a\hat{\mu}) \\ &\quad - U_\rho^\dagger(x - a\hat{\rho}) U_\mu(x - a\hat{\rho}) U_\rho(x - a\hat{\rho} + a\hat{\mu}))\end{aligned}\quad (4.23)$$

$$\begin{aligned}\delta_\rho^{(2)} U_\mu(x) &\equiv \frac{1}{a^2} (U_\rho(x + a\hat{\rho}) U_\rho^\dagger(x + a\hat{\mu}) \\ &\quad - 2U_\mu(x) \\ &\quad + U_\rho^\dagger(x - a\hat{\rho}) U_\mu(x - a\hat{\rho}) U_\rho(x - a\hat{\rho} + a\hat{\mu}))\end{aligned}\quad (4.24)$$

With this we can define the smearing operator;

$$\mathcal{F}_\mu = \prod_{\rho \neq \mu} \left(1 + \frac{a^2 \delta_\rho^{(2)}}{4} \right) \quad (4.25)$$

HISQ uses two different smeared gauge fields defined by;

$$X_\mu(x) \equiv \mathcal{U} \mathcal{F}_\mu U_\mu(x) \quad (4.26)$$

$$W_\mu(x) \equiv \left(\mathcal{F}_\mu - \sum_{\rho \neq \mu} \frac{a^2 (\delta_\rho)^2}{2} \right) \mathcal{U} \mathcal{F}_\mu U_\mu(x) \quad (4.27)$$

where \mathcal{U} is a re-unitarization operator. The HISQ action can then be written as:

$$S_{\text{HISQ}} = \sum_x \bar{\psi}(x) \left(\gamma \cdot \left(\nabla_\mu(W) - \frac{a^2}{6} (1 + \epsilon_{\text{Naik}}) \nabla_\mu^3(X) \right) + m \right) \psi(x) \quad (4.28)$$

Where $\nabla_\mu(Z)$ is the covariant derivative (4.8) with gauge links repaced with Z . This action in fact not only removes tree level interactions like fig. 4.1, but also all taste mixing interactions at 1-loop. The ∇_μ^3 term is introduced to remove "lattice artifacts", i.e. it reduces the size of $\mathcal{O}(a)$ terms in the $a \rightarrow 0$ limit of the action. In the same spirit, ϵ_{Naik} is fixed according to the constraint

$$\lim_{\underline{p} \rightarrow 0} \frac{E^2(\underline{p}) - m^2}{\underline{p}^2} = 1 \quad (4.29)$$

where $E(\underline{p})$ obeys the dispersion relation from HISQ. The motivation for the specific smearing of the gauge fields (4.27), and more details on HISQ in general, are given in [33].

4.3 Dealing with Heavy Quarks

heavy quarks are hard, because they fall inbetween lattice sites. b is almost within reach.

4.3.1 Heavy HISQ

extrapolation to physical b

general principles of fit function (hqed etc)

4.3.2 Lattice NRQCD

this can be done at the physical m_b , rest mass chopped out

write out lattice NRQCD action

define lattice NRQCD currents

Lattice Calculations

5.1 Correlation Functions from Lattice Simulations

A typical quantity that is computed on the lattice is a meson correlation function, i.e. when $\mathcal{O} = \Phi(x)\Phi^\dagger(y)$ and Φ is a meson creation operator. This is a good working example for showing the steps in a lattice calculation.

A creation operator for a meson in this context can be any operator containing the same quantum numbers as the meson one is trying to create. For example, the neutral B meson is a pseudoscalar charged with a d and \bar{b} quark, so a suitable operator is $\Phi(x) = \bar{b}(x)\gamma_5 d(x)$. The path integral can then be written as

$$C(x, y) = \int \mathcal{D}\psi \mathcal{D}\bar{\psi} \mathcal{D}U \left(\bar{b}(x)\gamma_5 d(x) \bar{d}(y)\gamma_5 b(y) \right) e^{-S_G[U] - \sum_{w,z} \bar{\psi}(w)M(w,z)[U]\psi(z)} \quad (5.1)$$

where we have now broken the action up into a gauge part $S_G[U]$, and a fermion part. $M(x, y)[U]$ is the Dirac operator, and can be seen as a matrix in lattice site, flavor, color and spin. ψ is a vector of quark flavours.

The integral over fermions can be preformed analytically, since the fermion fields are Grassman valued. In our example, the result is [34],

$$C(x, y) = \int \mathcal{D}U \text{Tr} \left[M_b^{-1}(y, x)[U] \gamma_5 M_d^{-1}(x, y)[U] \gamma_5 \right] e^{-S_G[U] \det(M[U])} \quad (5.2)$$

The quantities $M_f^{-1}(x, y)[U]$ are propagators of a quark of flavour f on a fixed gauge background U . The integration over gauge fields is generally carried out by an importance sampling method. A finite *ensemble* of gauge configurations $\{U_i\}$ is generated by a Monte Carlo Markov chain (MCMC), where the probability of a gauge configuration U_j being added to the ensemble is proportional to

$$e^{-S_G[U_j] \det(M[U])} \quad (5.3)$$

See [30] ch. 7 for examples of such algorithms. In the case of our work, we use ensembles generated by the MILC collaboration [35].

Once the ensemble is created, the path integral can be approximated by simply

$$C(x, y) \simeq \frac{1}{N} \sum_i \text{Tr} [M_b^{-1}(y, x) [U_i] \gamma_5 M_d^{-1}(x, y) [U_i] \gamma_5] \quad (5.4)$$

where N is the size of the ensemble. The calculation of the correlation function then is split into 3 steps:

1. Generate an ensemble of Gauge configurations $\{U_i\}$ by MCMC.
2. Compute quark propagators $M_f^{-1}(x, y)[U]$ on each Gauge configuration. This requires inverting the matrix M each time, this is typically done by conjugate gradient method.
3. Construct trace as in (5.4), and average over the ensemble.

We now turn to the issue of choosing lattice actions.

5.1.1 The Path Integral and Generation of Gauge Ensembles

discretise path integral

generate gauge configs using MCMC, breif review of options,
some detail of the option milc uses

5.1.2 Dirac Operator Inversion

conjugate gradient method

mass \simeq condition number \rightarrow light quarks are hard

5.1.3 Staggered Correlation Functions

introduce random wall sources

derive how 2-point functions look in terms of staggered propagators and phases.
similarly for 3-point functions, extended sources.

The full set of spin-mixing matrices can be labelled according to

$$\gamma_n = \prod_{\mu} (\gamma_{\mu})^{n_{\mu}} \quad n_{\mu} = \mathbb{Z}_2 \quad (5.5)$$

There are 16 such matrices representing corners of the hypercube. As $\gamma_\mu^2 = 1$, one can also use a general site vector x_μ to label the matrix, then $\gamma_x = \gamma_n$ where $n_\mu = x_\mu \bmod 2$. One can show that for any x ; $\gamma_x^\dagger \gamma_x = 1$.

Naive quarks $\psi(x)$ can be transformed into staggered quarks $\chi(x)$ via $\psi(x) = \gamma_x \chi(x)$. Then, Naive quark propagators (inverse Dirac operators) become

$$G_\psi(x, y) = \gamma_x \gamma_y^\dagger G_\psi(x, y) \quad (5.6)$$

By conjugating both sides and using γ_5 -hermiticity $G_\psi^\dagger(y, x) = \gamma_5 G_\psi(y, x) \gamma_5$ it can be shown that

$$G_\psi(x, y) = \phi_5(x) \phi_5(y) G_\psi^\dagger(y, x) \quad (5.7)$$

where $\phi_5(x) = (-1)^{\sum_\mu x_\mu}$.

2pt correlation functions

We will break down the correlation function to see what quantities must be computed by the simulation. Consider the generic 2-point correlator:

$$C(x, y) = \langle \Phi_X^\dagger(x) \Phi_Y(y) \rangle_{\psi, U} \quad , \quad \Phi_X(x) = \frac{1}{4} \bar{\psi}_a(x) \gamma_X \psi_b(x) \quad (5.8)$$

$$= \frac{1}{16} \langle tr_{c,s} \gamma_X G_{a,\psi}(x, y) \gamma_Y G_{b,\psi}(y, x) \rangle_U \quad (5.9)$$

$$= \frac{1}{16} tr_s \left(\gamma_x^\dagger \gamma_X \gamma_x \gamma_y^\dagger \gamma_Y \gamma_y \right) \langle tr_c (G_{a,\chi}(x, y) G_{b,\chi}(y, x)) \rangle_U \quad (5.10)$$

tr_s is a trace over spin and tr_c is over colour. To deal with the spin trace, define the family of phases $\{\phi_X(x)\}$ according to

$$\gamma_x^\dagger \gamma_X \gamma_x = \phi_X(x) \gamma_X \quad (5.11)$$

for example, if $X = 5$, then $\gamma_x^\dagger \gamma_5 \gamma_x = (-1)^{\sum_\mu x_\mu} \gamma_x^\dagger \gamma_x \gamma_5 = \phi_5(x) \gamma_5$. The map from X to ϕ_X is structure preserving, i.e. if $\gamma_X = \gamma_A \gamma_B$, then $\phi_X(x) = \phi_A(x) \phi_B(x)$. The spin trace becomes $\phi_X(x) \phi_Y(y) tr_s (\gamma_X \gamma_Y)$. The will vanish unless $Y = X$, as one would expect physically for the correlation function. We end up with

$$C(x, y) = \frac{1}{4} \phi_X(x) \phi_X(y) \langle tr_c G_{a,\chi}(x, y) G_{b,\chi}(y, x) \rangle_U \quad (5.12)$$

It is useful in the simulation to replace $G_{b,\chi}(y, x)$ with it's conjugate via (5.7), resulting in

$$C(x, y) = \frac{1}{4} \phi_{5X}(x) \phi_{5X}(y) \langle tr_c G_{a,\chi}(x, y) G_{b,\chi}^\dagger(y, x) \rangle_U \quad (5.13)$$

where $\phi_{5X}(x) = \phi_5(x)\phi_X(x)$. To obtain the correlation function of a meson in an eigenstate with momentum \underline{p} , the above must be replaced with

$$C_{\underline{p}}(t_0, t) = \frac{1}{L^3} \sum_{\underline{x}, \underline{y}} e^{i\underline{p} \cdot (\underline{x} - \underline{y})} C(\underline{x}, t_0; \underline{y}, t) \quad (5.14)$$

$$= \frac{1}{4L^3} \sum_{\underline{x}, \underline{y}} e^{i\underline{p} \cdot (\underline{x} - \underline{y})} \phi_{5X}(x) \phi_{5X}(y) \langle \text{tr}_c G_{a,\chi}(x, y) G_{b,\chi}^\dagger(y, x) \rangle_U, \quad (5.15)$$

where it is understood that $x_0 = t_0$ and $y_0 = t$. In order to evaluate this function, the simulation must perform inversions to create $G_{a/b,\chi}(x, y)$ for each x and y , so $2 \cdot \text{Vol}^2$ operations. This is prohibitively expensive. The number of inversions can be reduced using *random wall sources*. Define

$$P_{a,\underline{p},X}^{t_0}(y) \equiv \frac{1}{\sqrt{L^3}} \sum_{\underline{x}} e^{i\underline{p} \cdot (\underline{x} - \underline{y})} \phi_{5X}(\underline{x}, t_0) \xi(\underline{x}) G_{a,\chi}(\underline{x}, t_0; y), \quad (5.16)$$

where $\xi(\underline{x})$ is a random field of colour vectors, varying with U . This has the property

$$\langle f(\underline{x}, \underline{x}') \xi^*(\underline{x}') \xi(\underline{x}) \rangle_U = \delta_{\underline{x}, \underline{y}} \langle f(\underline{x}, \underline{y}) \rangle_U. \quad (5.17)$$

Using this property it can be shown that the correlator can be build instead according to

$$C(\underline{x}, t_0; \underline{y}, t) \simeq \frac{1}{4} \sum_{\underline{y}} \phi_{5X}(y) \langle \text{tr}_c P_{a,\underline{p},X}^{t_0}(\underline{y}, t) P_{b,\underline{0},1}^{t_0,\dagger}(\underline{y}, t) \rangle_U \quad (5.18)$$

Now all the simulation has to do is compute $P_{a/b}^{t_0}(y)$ for general y , so $2 \cdot \text{Vol}$ operations, a reduction by a factor of Vol .

In the MILC code, "sources" are first created (the fields $\phi_{5X}(\underline{x}, t_0) \xi(\underline{x})$), then the objects $P^{t_0}(y)$ (referred to as "propagators") are generated from them. Any extra factors dependant on y (this is useful for "smeared" propagators, see ?) can be multiplied in. The resulting object $f(y) \cdot P^{t_0}(y)$ is referred to as a "quark". Finally, two of these quarks can be "tied together" according to (5.18), to produce correlation functions. The sources are chosen to be on some single timeslice t_0 , resulting in a value for $C(t_0, t)$ at each t .

The above discussion can be generalized to 3—(or N —)point correlation functions using *extended sources*. Consider a 3-pt correlator encoding the form-factors of a semileptonic decay from meson X to meson Z , via a current J . We start by

evaluating

$$\begin{aligned} C(x, y, z) &= \langle \Phi_X^\dagger(x) J(y) \Phi_Z(z) \rangle_{\psi, U} \quad , \quad \Phi_X(x) = \frac{1}{4} \bar{\psi}_b(x) \gamma_X \psi_s(x) \\ J(y) &= \bar{\psi}_b(y) \gamma_J \psi_a(y) \\ \Phi_Z(z) &= \frac{1}{4} \bar{\psi}_a(z) \gamma_Z \psi_s(z) \end{aligned} \quad (5.19)$$

in the same way as before:

$$C(x, y, z) = \frac{1}{16} \text{tr}_s \left(\gamma_x^\dagger \gamma_X \gamma_x \gamma_y^\dagger \gamma_J \gamma_y \gamma_z^\dagger \gamma_Z \gamma_z \right) \langle \text{tr}_c G_{b,\chi}(x, y) G_{a,\chi}(y, z) G_{s,\chi}(z, x) \rangle_U \quad (5.20)$$

$$= \frac{1}{4} \phi_{5X}(x) \phi_J(y) \phi_{5Z}(z) \langle \text{tr}_c G_{b,\chi}(x, y) G_{a,\chi}(y, z) G_{s,\chi}^\dagger(z, x) \rangle_U \quad (5.21)$$

We have assumed that $\text{tr}_s \gamma_X \gamma_J \gamma_Z = 4$, requiring that each gamma matrix in this combination has a partner and therefore cancels. In any other situation the trace would vanish. For example, if the current is a temporal vector $J = 0$, and the two mesons represent pseudoscalars, one of the meson operators must have a γ_0 , i.e. one could choose $\gamma_X = \gamma_0 \gamma_5, \gamma_Z = \gamma_5$. **why is it ok to have a non-goldstone for X ?**

Putting X into an eigenstate of zero momentum, and Y into an eigenstate of momentum \underline{p} , we get

$$C_{\underline{p}}(t_0, t, T) = \frac{1}{4L^3} \sum_{\underline{x}, \underline{y}, \underline{z}} e^{i\underline{p} \cdot (\underline{y} - \underline{z})} \phi_{5X}(x) \phi_J(y) \phi_{5Z}(z) \langle \text{tr}_c G_{b,\chi}(\underline{x}, t_0; \underline{y}, t) G_{a,\chi}(\underline{y}, t, \underline{z}, T) G_{s,\chi}^\dagger(\underline{z}, T; \underline{x}, t_0) \rangle_U \quad (5.22)$$

This can be built by first creating propagators for the b and s quarks: $P_{b,0,X}^{t_0}(y), P_{s,0,1}^{t_0}(z)$. Then, build the a propagator using an extended source, i.e.:

$$P_{a,\underline{p},ext}^T(y) = \sum_{\underline{z}} P_{s,0,1}^{t_0}(\underline{z}, T) \phi_{5Z}(\underline{z}, T) G_{a,\chi}(\underline{z}, T; y) \quad (5.23)$$

Then, by plugging $P_{b,0,X}^{t_0}(y)$ and $P_{a,\underline{p},ext}^T(y)$ into the MILC tie-together defined by (5.18), one ends up evaluating (5.22).

Momentum Twist

The momentum space 2-point correlation function for an operator \mathcal{O} with external momentum \underline{p} is given by

$$C(\underline{p}, t) = \sum_{\underline{x}} e^{i\underline{p} \cdot \underline{x}} \langle \mathcal{O}^\dagger(\underline{x}, t) \mathcal{O}(\underline{0}, 0) \rangle \quad (5.24)$$

To extend the method for computing zero momentum correlators to non-zero, one can compute $S(\underline{0}, t)$ with rephased operators, exploiting the fact that

$$\mathcal{O}(\underline{x}, t) \rightarrow \mathcal{O}(\underline{x}, t) e^{-i\underline{p} \cdot \underline{x}} \quad (5.25)$$

$$\implies C(\underline{0}, t) \rightarrow C(\underline{p}, t) \quad (5.26)$$

This generalised straightforwardly to n -point functions. One can assign the rephasing to any factor in \mathcal{O} , for example a fermion operator

$$\psi(\underline{x}, t) \rightarrow \psi(\underline{x}, t) e^{-i\underline{p} \cdot \underline{x}} \quad (5.27)$$

Rephasing ψ is equivalent to introducing the so-called *momentum twist* to the gauge links. The action of (5.25) on any gauge invariant quantity is equivalent to

$$U_i \rightarrow U_i e^{ip_i} \quad (\text{no sum}) \quad (5.28)$$

proof(ish)

$$\psi^\dagger(x) U_\mu(x) U_\nu(x + \mu) \psi(x + \mu + \nu) \quad (5.29)$$

$$\rightarrow \psi^\dagger(x) U_\mu(x) U_\nu(x + \mu) e^{i(p_\mu + p_\nu)} \psi(x + \mu + \nu) \quad (5.30)$$

$$= \psi^\dagger(x) (e^{ip_\mu} U_\mu(x)) (e^{ip_\nu} U_\nu(x + \mu)) \psi(x + \mu + \nu) \quad (5.31)$$

As an aside, this can be seen as coupling ψ to an additional $U(1)$ gauge field A_μ , with constant value $A_\mu = (0, \underline{p})$ (ref!).

(5.28) is how external momenta is simulated in lattice simulations. In the case of multiple fermion fields, where we want to rephase some and not others (or different rephasings), care must be taken to only give the links a twist when in terms including the appropriate fermion.

5.2 Analysis of Correlation Functions

derive the fit function for correlation functions, 2-point and 3-point

how fit parameters relate to energies, decay constants, transition matrix elements...

5.2.1 Non-Linear Regression

Levenberg-Marquardt algorithm

Bayesian constraining of fits

general rules for priors

Once a correlation function like the in ?? has been computed, we can extract physics from it, namely the mass and decay constant of the meson we are studying. In practice the meson creation operators defined above are fourier transformed

$$\Phi(\underline{k}, t) = \sum_{\underline{x}} e^{-i\underline{k} \cdot \underline{x}} \Phi(\underline{x}, t) \quad (5.32)$$

which serves to change (5.4) into

$$C_{\underline{k}}(t) = \frac{1}{N} \sum_i \sum_{\underline{x}, \underline{y}} e^{-i\underline{k} \cdot (\underline{x} - \underline{y})} \text{Tr} [M_b^{-1}(\underline{y}, t; \underline{x}, 0) [U_i] \gamma_5 M_d^{-1}(\underline{x}, 0; \underline{y}, t) [U_i] \gamma_5] \quad (5.33)$$

(5.33) is computed for many t values with a lattice calculation following the principles detailed above. One performs a least-squares fit of this to a theoretically motivated function of t . To derive such a function, first construct a complete set of momentum \underline{k} states with quantum numbers matching the meson:

$$1 = \sum_{n=0} \frac{1}{2E_n^r} |\lambda_n\rangle \langle \lambda_n|. \quad (5.34)$$

Where $E_n^r = \sqrt{M_n^2 + \underline{k}^2}$ are the relativistic energies of each state. Inserting this into the correlation function, and moving from the Heisenberg to Schroedinger picture;

$$\begin{aligned} C_{\underline{k}}(t) &= \sum_{n=0} \frac{1}{2E_n^r} \langle 0 | e^{Ht} \Phi(\underline{k}, 0) e^{-Ht} | \lambda_n \rangle \langle \lambda_n | \Phi^\dagger(\underline{k}, 0) | 0 \rangle \\ &= \sum_{n=0} \left(\frac{\langle 0 | \Phi(\underline{k}, 0) | \lambda_n \rangle}{\sqrt{2E_n^r}} \right) \left(\frac{\langle \lambda_n | \Phi^\dagger(\underline{k}, 0) | 0 \rangle}{\sqrt{2E_n^r}} \right) e^{-E_n^l t} \\ &\equiv \sum_{n=0} |a_n|^2 e^{-E_n^l t}. \end{aligned} \quad (5.35)$$

The fit results in a determination of the parameters a_n , and E_n^l . Since the lowest energies dominate the function at late times, one can afford to truncate the sum over n to some tractable range, in our case $n \in [1, 6]$. We interpret $|\lambda_0\rangle$ to be the ground state of the meson we are studying. The exponential decays mean the fit function is dominated by the ground state at large t , and subsequent excited states

become less important as E_n^l increases. Hence by only including $C_{\underline{k}}(t)$ at suitably large t values, we can afford to truncate the sum in n . In our fits we chose $n = 6$.

We maintain a distinction between E^l and E^r , since for example in simulations involving NRQCD quarks these differ. If this is not an issue, as is the case with HISQ, one can compute the correlation function at zero momentum $C_0(t)$, then fit it to find the parameter E_0^l , which will equal the meson's mass M . Noting the definition of a meson decay constant f : $\langle 0 | J_0 | \text{Meson}(\underline{k} = 0) \rangle = Mf$, where J_0 is a temporal current with the same quantum numbers as the meson, we can see that the fit parameters a_n at zero momentum are related to the meson's decay constant via

$$f = \sqrt{\frac{2}{M}} a_0 \quad (5.36)$$

Hence the fit can also be used to extract decay constants.

The above discussion can be straightforwardly generalized to 3-point correlation functions, from which we are able to extract quantities like the hadronic transition amplitudes $H_\mu = \langle M_{q_1 \bar{q}_3} | J_\mu^{q_1 \bar{q}_2} | M_{q_2 \bar{q}_2} \rangle$ from sec. ???. Specifically the quantity we require in order to deduce the $B_s \rightarrow D_s l \nu$ form factors is $\langle D_s | V_\mu | B_s \rangle$, where $V_\mu = \bar{c} \gamma_\mu b$.

The generalization of the above for 3pt functions is summarized here:

$$C_3(t, T) = \int \mathcal{D}\psi \mathcal{D}\bar{\psi} \mathcal{D}U \left(\Phi_{D_s}(\underline{0}, 0) V_\mu(-\underline{p}, t) \Phi_{B_s}^\dagger(\underline{p}, T) \right) e^{-S[\psi, \bar{\psi}, U]} \quad (5.37)$$

$$\simeq \frac{1}{N} \sum_i \sum_{\underline{x}, \underline{y}, \underline{z}} e^{-i\underline{p} \cdot (\underline{y} - \underline{z})} \text{Tr} \left[M_b^{-1}(\underline{x}, 0; \underline{y}, t) [U_i] \gamma_\mu M_c^{-1}(\underline{y}, t; \underline{z}, T) [U_i] \gamma_5 \gamma_5 M_s^{-1\dagger}(\underline{z}, T; \underline{x}, 0) [U_i] \right] \quad (5.38)$$

$$= \sum_{n, m} \left(\frac{\langle 0 | \Phi_{D_s} | \lambda_n \rangle}{\sqrt{2E_n^r}} \right) \left(\frac{\langle \lambda_n | V_\mu | \lambda_m \rangle}{2\sqrt{E_n^r E_m^r}} \right) \left(\frac{\langle \lambda_m | \Phi_{B_s}^\dagger | 0 \rangle}{\sqrt{2E_m^r}} \right) e^{-E_m^l(T-t)} e^{-E_n^l t} \quad (5.39)$$

$$\equiv \sum_{n, m} a_{D_s, n} V_{nm} a_{B_s, m}^* e^{-E_m^l(T-t)} e^{-E_n^l t}.$$

$C(t, T)$ is computed at different values of t and T , then a least-squares fit is performed to the fit function (5.40). a_n will vanish for states $|\lambda_n\rangle$ which have different quantum numbers to Φ_{B_s} , and similarly for b_m and Φ_{D_s} . Non-zero a_n 's will match

the analogous parameters extracted from fitting a 2pt function $\langle \Phi_{B_s}^\dagger \Phi_{B_s} \rangle$, similarly for b_n 's and Φ_{D_s} . This carries on to the energies, $\{E_n^l\}$ is the spectrum for the D_s meson, and $\{E_m^l\}$ is the spectrum for the B_s . Therefore, we compute and fit the appropriate 2pt functions to deduce the parameters $\{a_n\}, \{b_m\}, \{E_n^l\}$. Then, fitting $C_3(t, T)$ results in an accurate determination of the remaining free parameters, V_{nm} . This set contains the quantity we need, recognising that:

$$V_{00} = \frac{\langle D_s | V_\mu | B_s \rangle}{2\sqrt{E^{B_s} E^{D_s}}} \quad (5.40)$$

2-point correlation functions are then fitted as in sec. ???. The fit function we use is modified a little from (5.35), we use:

$$\begin{aligned} C^{\alpha\beta}(t) = & \sum_n a_n^{\alpha*} a_n^\beta (e^{-E_n^l t} - s e^{-E_n^l (T-t)}) \\ & + \sum_n a_n'^{\alpha*} a_n'^\beta (-1)^t (e^{-E_n'^l t} - s e^{-E_n'^l (T-t)}) \end{aligned} \quad (5.41)$$

Firstly, the parameters $\{a_n\}$ must vary between source and sink to account for the different operators. Secondly, the periodicity of the lattice in the time direction means an extra exponential term is required, but not in the case of the B_s since NRQCD quarks do not experience the periodicity of the lattice. Hence s is set to 0 for the B_s correlator and 1 for the D_s . T is the time extent of the lattice. The second term is to account for the so-called "oscillating state", which is in fact the $\zeta = (1, 0, 0, 0)$ doubler fermion appearing due to the doubling in the HISQ action (see sec. 4.15). No other doublers contribute, since $\Phi_{\underline{k}}$ has a 3-momentum fixed at \underline{k} , which we always take to be small relative to π/a , hence does not couple to the states at $k \sim (0, \pi/a, 0, 0)$, $k \sim (0, 0, \pi/a, 0)$ etc. However, $\Phi_{\underline{k}}$ can couple to arbitrarily high energy states, so the $k \sim (\pi/a, 0, 0, 0)$ doubler contributes. The second term in (5.41) is justified by performing the doubling operation \mathcal{B}_0 defined in (5.35), the quark fields in $\Phi_{\underline{k}}$ which obey the HISQ action. See appendix G of [33] for details.

We use the *CorrFitter* package [36] for performing Bayesian least-squares fitting to the correlation functions. The package employs the trust region method of least-squares fitting. The fits require priors for each of the fit parameters. The "amplitude" parameters $a_{n,B_s/D_s}^\alpha$ are given priors of 0.1(1.0), thus inserting only the assumption that they are of $\mathcal{O}(1)$. The ground state energies are given priors motivated by the meson masses, and excited state energies are given loose, evenly

spaced priors with 600MeV between each level.

2-point correlation functions for B_s and D_s are fit to (5.41), resulting in $a_{n,B_s/D_s}^\alpha, E_{n,B_s/D_s}^l$. Since the HISQ action is fully relativistic, E_{0,D_s}^l at $\underline{k} = 0$ can be interpreted as the D_s meson mass. The same cannot be done for the B_s . The decay constants for B_s and D_s can be deduced from a_{0,B_s}^0 and a_{0,D_s}^0 , since Φ_{B_s,D_s}^0 are also temporal axial currents. This is a good avenue for consistency checks, we compared $M_{D,s}, f_{D_s}$ and f_{B_s} to those computed in [37], [16] amongst others, and found them to be consistent (modulo small shifts we can reasonably expect due to differing choices of bare quark masses).

We now discuss fitting the 3-point correlation functions. The same considerations as those that went into (5.41) lead us to our 3-point fit function:

$$\begin{aligned}
C_3^{\alpha\beta}(t, T) = & \sum_{k,m} (a_{k,D_s}^\alpha V_{km}^{nn} a_{m,B_s}^{*\beta} e^{-E_m^l t} e^{-E_k^l (T-t)} \\
& + a_{k,D_s}^\alpha V_{km}^{no} a_{m,B_s}^{'*\beta} e^{-E_m^l t} e^{-E_k^l (T-t)} \\
& + a_{k,D_s}^{'\alpha} V_{km}^{on} a_{m,B_s}^{*\beta} e^{-E_m^l t} e^{-E_k^l (T-t)} \\
& + a_{k,D_s}^{'\alpha} V_{km}^{oo} a_{m,B_s}^{'*\beta} e^{-E_m^l t} e^{-E_k^l (T-t)}) \quad (5.42)
\end{aligned}$$

The 2-point and 3-point correlators are fit simultaneously, according to fit functions (5.41) and (5.42). The parameters involved in the 2pt fits are mostly fixed by the data in the 2pt correlation functions, so the fit can use most of the data in the 3pt correlation functions to determine the transition amplitudes V_{km}^{ab} . This is carried out for each B_s and D_s smearing, each direction μ and each current correction i of the vector current $V_\mu^{(i)}$.

In this large 2pt/3pt fit, there is a huge χ^2 manifold with many local minima, and it is crucial to impose strong priors in order to ensure the fit finds the true minimum. Priors for ground state 2-point amplitudes and energies $a_{0,B_s/D_s}^\alpha, E_{0,B_s/D_s}^l$ are taken to be the results from individual fits of the 2-point functions, with the errors expanded by a factor of 2. The excited state amplitudes and energies are given the same priors as in the 2-point fits. The transition amplitudes V_{km}^{ab} are given the prior 0.1(1.0), assuming it to be $\mathcal{O}(1)$.

Finally, we end up with the sought-after parameters V_{00}^{nn} representing $V_\mu^{(i)}$,

via the relation

$$\langle D_s | V_\mu^{(i)} | B_s \rangle = 2\sqrt{M^{B_s} E^{D_s}} V_{00}^{nn} |_{V=V_\mu^{(i)} \text{ in simulation}} \quad (5.43)$$

We have asserted the ground state of B_s to be it's mass, but not the D_s , as we give D_s spacial momenta in the calculation (to be expanded on in the next section). Then, the full vector currents $\langle D_s | V_\mu^{(i)} | B_s \rangle$ can be build from a linear combination of these according to ??.

5.2.2 The Golden Window

explanation of why t_{cut} is neccesary.

signal/noise degradation as t gets bigger in presence of heavy things or high momenta

One of the main obstacles in our calculation is the *signal degradation* of correlation functions computed on the lattice.

A random variable x has mean and standard deviation

$$\hat{x} = \langle x \rangle \quad (5.44)$$

$$\sigma^2 = \frac{1}{N} (\langle x^2 \rangle - \langle x \rangle^2), \quad (5.45)$$

where N is the size of the sample. So the (square of) the signal/noise ratio is

$$\frac{\hat{x}^2}{\sigma^2} = N \left(\frac{\langle x^2 \rangle}{\langle x \rangle^2} - 1 \right)^{-1}. \quad (5.46)$$

Consider 2 point correlators where $x = \Phi^\dagger(t)\Phi(0)$, where Φ is a meson operator with zero spacial momentum.

$\langle x^2 \rangle$ and $\langle x \rangle$ can be written as

$$\langle x \rangle = \sum_k \frac{1}{2E_n} \langle 0 | \Phi^\dagger(t) | \lambda_n \rangle \langle \lambda_n | \Phi(0) | 0 \rangle e^{-E_n t} \simeq_{t \rightarrow \infty} e^{-E_0 t} \quad (5.47)$$

$$\langle x^2 \rangle = \sum_n \frac{1}{2E_n} \langle 0 | \Phi^{\dagger 2}(t) | \lambda_n \rangle \langle \lambda_n | \Phi^2(0) | 0 \rangle e^{-E_n t} \simeq_{t \rightarrow \infty} e^{-E'_0 t} \quad (5.48)$$

where we have assumed the ratio of matrix elements and energies are $\mathcal{O}(1)$. The two ground state energies E_0 and E'_0 need not be the same, since the lowest states for which $\langle \lambda_n | \Phi(0) | 0 \rangle \neq 0$ and $\langle \lambda_n | \Phi^2(0) | 0 \rangle \neq 0$ may differ.

The operator Φ^2 will contain two quark and two antiquark operators, connected by some matrices in spin space. Φ^2 can create a combination of all possible 2 meson states where the mesons are made of the available quark species, and quantum numbers. For example, If Φ is a pion, Φ^2 is a 2 pion state, and $E'_0 = 2m_\pi$. If Φ is a D_s meson, then $E'_0 = m_{\tilde{\pi}} + m_{\eta_c}$ ($\tilde{\pi}$ is a pseudoscalar $s\bar{s}$ state).

Define $\mu_0 = E'_0/2$. Then

$$\frac{\hat{x}^2}{\sigma^2} \simeq N \left(e^{-2(\mu_0 - m_\Phi)t} - 1 \right)^{-1} \quad (5.49)$$

In the case of pions, $\mu_0 = m_\Phi$, the ratio becomes simply $\sim N$. For mesons heavier than the pion, $\mu_0 < m_\Phi$, so at large times $e^{-2(\mu_0 - m_\Phi)t} \gg 1$, and upon taylor expanding the inverse of this phase we arrive at

$$\frac{\hat{x}}{\sigma} \simeq \sqrt{N} e^{-(m_\Phi - \mu_0)t} \quad (5.50)$$

From this we see there are 3 variables which effect the quality of the signal:

1. The size of the sample N .
2. At large t , the correlators undergo *signal degradation*, i.e, become dominated by noise.
3. The degree of signal degradation is decided by $m_\Phi - \mu_0$. Heavier mesons will tend to experience more signal degradation.

Relevant to our calculation is how giving mesons non-zero spacial momenta \underline{p} can exaserbate this problem. In this case, m_Φ in (5.50) is replaced with $\sqrt{m_\Phi^2 + \underline{p}^2}$. As \underline{p} increases, the signal/noise ratio will degrade more and more and statistics will suffer.

In the $B_s \rightarrow D_s l \nu$ calculation, to deduce form factors over the whole range of q^2 values, we need to simulate the process with the D_s having a range of momenta $0 < |\underline{p}| < 2.32\text{GeV}$, as discussed in sec. ???. Correlation functions at the higher end of this range may be too noisy for any meaningful results to be extracted. We are investigating ways of taming this problem, see sec. ???.

5.3 Renormalization of Currents

general principle of matching factors

Once one has computed a matrix element from a lattice calculation, it needs to be translated into a continuum regularization scheme. Suppose we have some bare operator \mathcal{O}_0 , we expect this to be related to the renormalized operator in \overline{MS} at scale μ , $\mathcal{O}^{\overline{MS}}(\mu)$, via

$$\mathcal{O}^{\overline{MS}}(\mu) = Z^{\overline{MS}}(\mu) \mathcal{O}_0. \quad (5.51)$$

Similarly, in a lattice regularization,

$$\mathcal{O}^{\text{lat}}(1/a) = Z^{\text{lat}}(1/a) \mathcal{O}_0. \quad (5.52)$$

Hence we expect a multiplicative factor between the lattice matrix elements, and the continuum \overline{MS} ones:

$$\langle \mathcal{O} \rangle^{\overline{MS}} = \mathcal{Z}(\mu, 1/a) \langle \mathcal{O} \rangle^{\text{lat}} \quad (5.53)$$

where $\mathcal{Z}(\mu, 1/a) = Z^{\overline{MS}}(\mu)/Z^{\text{lat}}(1/a)$. These "matching factors" \mathcal{Z} can be deduced by equating observables calculated in both lattice QCD and continuum (appropriately regularized) QCD, producing equations which can be solved for \mathcal{Z} . The lattice side of the calculation can be done either through lattice perturbation theory ("perturbative matching"), or through a simulation ("non-perturbative matching").

It is a well-known result that conserved (or partially conserved) currents do not receive any renormalization in any scheme, i.e. $Z^{\text{any}} = 1$ ("absolutely normalized").

In principle this is of great help, since the currents we are calculating, namely V_μ , are partially conserved, so we are not required to include any matching factors. However in practice, this is complicated by the fact that the conserved current in the lattice theory is often computationally difficult or impossible to compute. For example, in NRQCD, the partially conserved current corresponding to $SU(N)_V$ is an infinite sum in $1/m_b$ where m_b is the bottom mass. The corresponding current in HISQ is also the sum of a large number of operators. This can be interpreted as a mixing in the renormalization:

$$\langle \mathcal{O}_i \rangle^{\overline{MS}} = \mathcal{Z}_{i,j} \langle \mathcal{O}_j \rangle^{\text{lat}} \quad (5.54)$$

In practice, lattice calculations often use only the dominant operators that contribute to the conserved current. Since these will be "close" to the conserved current, one can expect the matching factor to only be a small deviation from unity,

and the more sub-dominant operators you add, the overall matching factor should tend towards one.

5.3.1 Non-perturbative Renormalization of HISQ Currents

$(m_1 - m_2)S$ absolutely normalised,
 V, A normalisations via ward identities

5.3.2 Matching NRQCD currents to \overline{MS}

list currently available matching factors,
 mention what isn't available, where we need to truncate the series of currents,
 the issues this brings up.

b -Physics from Lattice NRQCD

6.1 $B_{(s)} \rightarrow D_{(s)} l \nu$ Form Factors

breif motivation

disclaimer: this was never properly finished! (is it ok to say this?)

6.1.1 Calculation Setup

ensemble details, what correlators were calculated, etc.

6.1.2 Results

as far as I got : plots of form factors

discuss how too many correlators makes the fits very unstable...

6.1.3 The Subleading Current Problem

Talk about the fact that $J_k^{(3,4)}$ are huge, how there isn't much way around this

6.2 Nonperturbative Renormalisation

6.2.1 Relativistic Normalisation of the $b \rightarrow c$ Axial Current

brief description of what we were trying to do: test normalisations, or fix new normalisations

results - plots of $a_0(p)/a_0(0)$ against p^2

why it didn't work

6.2.2 $b \rightarrow c$ Vector Current Matching to Heavy-HISQ

Explain that $B_c \rightarrow \eta_c$ data from both heavy-HISQ and NRQCD were available, ref. Andrew & Brian.

Fix normalisation of V_0 by comparing f_0/f_{B_c} at zero recoil at $q^2 = 0$.

$B_s \rightarrow D_s^* l \nu$ Axial Form Factor at Zero Recoil from Heavy-HISQ

brief motivation, V_{cb} etc.

7.1 Calculation Setup

ensembles, masses, etc. used

basically going to repurpose paper in here

7.2 Results

7.3 Implications for $B \rightarrow D^* l \nu$ and $|V_{cb}|$

$B \rightarrow D^*$, fermilab data plot, how it relates to $|V_{cb}|$ tensions etc.

$B_s \rightarrow D_s l \nu$ Form Factor at All Physical q^2 from Heavy-HISQ

brief motivation, V_{cb} etc.

8.1 Calculation Setup

basically repurpose paper again

8.2 Results

8.3 HQET low energy constants

won't mention this in the paper, but i did some work fitting h_+ to the HQET expression, similar to in the $Bs - Ds^*$ case

List of Figures

2.1	The flavour-changing charged current vertex.	7
2.2	A sketch of the unitarity triangle.	10
2.3	Exclusion regions for the vertices of the CKM triangle from various measurements, courtesy of the most recent PDG update [!]	11
2.4	Leptonic decay of meson M at tree level in the electroweak coupling.	12
2.5	Semileptonic decay, $M \rightarrow M' l \bar{\nu}$, at tree level in electroweak coupling.	13
2.6	Different determinations of $ V_{cb} $. Points labelled $w = 1$ are determinations from extrapolating measurements of decay rates to the zero recoil point, and combined with a lattice determination of the form factor at zero recoil. Points labelled $w \geq 1$ are results from using a combination of both branching fractions and lattice form factors through some range of w . The first name mentioned in the labels give the source of the lattice form factors, and the second gives the source of the experimental data (e.g. the HPQCD+BaBar point used form factors from the HPQCD collaboration and data from the BaBar experiment. The highest point is from [5], the second and third highest from [6], fourth from [7], fifth from [8]. The bottom point is from the PDG [1], using data from the ALPEPH [9], Belle [10], BaBar [11,12], and CLEO [13] experiments.	16
2.7	$R(D)/R(D^*)$ determinations from standard model and experiment [?]	19
3.1	The relationship between scale Q and the strong coupling constant α_s , from the Particle Data Group [?]	22
4.1	Taste mixing at tree level.	42

List of Tables

Bibliography

- [1] M. et. al. Tanabashi. Review of particle physics. *Phys. Rev. D*, 98:030001, Aug 2018.
- [2] Bugra Borasoy. Introduction to Chiral Perturbation Theory. *Springer Proc. Phys.*, 118:1–26, 2008.
- [3] Ikaros I. Y. Bigi, Mikhail A. Shifman, N. Uraltsev, and Arkady I. Vainshtein. High power n of m_b in beauty widths and $n = 5 \rightarrow \infty$ limit. *Phys. Rev.*, D56:4017–4030, 1997. [,205(1996)].
- [4] Andre H. Hoang, Zoltan Ligeti, and Aneesh V. Manohar. B decays in the upslon expansion. *Phys. Rev.*, D59:074017, 1999.
- [5] Heechang Na, Chris M. Bouchard, G. Peter Lepage, Chris Monahan, and Junko Shigemitsu. $B \rightarrow D\ell\nu$ form factors at nonzero recoil and extraction of $|V_{cb}|$. *Phys. Rev.*, D92(5):054510, 2015. [Erratum: *Phys. Rev.*D93,no.11,119906(2016)].
- [6] Jon A. Bailey et al. $B \rightarrow D\ell\nu$ form factors at nonzero recoil and $|V_{cb}|$ from 2+1-flavor lattice QCD. *Phys. Rev.*, D92(3):034506, 2015.
- [7] Jon A. Bailey et al. Update of $|V_{cb}|$ from the $\bar{B} \rightarrow D^*\ell\bar{\nu}$ form factor at zero recoil with three-flavor lattice QCD. *Phys. Rev.*, D89(11):114504, 2014.
- [8] Benjamin Grinstein and Andrew Kobach. Model-Independent Extraction of $|V_{cb}|$ from $\bar{B} \rightarrow D^*\ell\bar{\nu}$. *Phys. Lett.*, B771:359–364, 2017.
- [9] D Buskulic et. al. A measurement of $|v_{cb}|$ from $b^0 \rightarrow d^*l^-\nu_l$. *Physics Letters B*, 359(1):236 – 248, 1995.
- [10] Kazuo Abe et al. Measurement of $B(\text{anti-}B^0 \rightarrow D + l + \text{anti-}\nu)$ and determination of $|V_{cb}|$. *Phys. Lett.*, B526:258–268, 2002.
- [11] Bernard Aubert et al. Measurements of the Semileptonic Decays $\text{anti-}B \rightarrow D + l + \text{anti-}\nu$ and $\text{anti-}B \rightarrow D^* + l + \text{anti-}\nu$ Using a Global Fit to $D + X + l + \text{anti-}\nu$ Final States. *Phys. Rev.*, D79:012002, 2009.

- [12] Bernard Aubert et al. Measurement of $|V(cb)|$ and the Form-Factor Slope in $B \rightarrow D^* \ell^- \bar{\nu}_\ell$ anti- ν Decays in Events Tagged by a Fully Reconstructed B Meson. *Phys. Rev. Lett.*, 104:011802, 2010.
- [13] John E. Bartelt et al. Measurement of the $B \rightarrow D^* \ell^- \bar{\nu}_\ell$ lepton neutrino branching fractions and form-factor. *Phys. Rev. Lett.*, 82:3746, 1999.
- [14] Dante Bigi, Paolo Gambino, and Stefan Schacht. A fresh look at the determination of $|V_{cb}|$ from $B \rightarrow D^* \ell \nu$. *Phys. Lett.*, B769:441–445, 2017.
- [15] Roel Aaij et al. Measurement of the ratio of branching fractions $\mathcal{B}(\bar{B}^0 \rightarrow D^{*+} \tau^- \bar{\nu}_\tau) / \mathcal{B}(\bar{B}^0 \rightarrow D^{*+} \mu^- \bar{\nu}_\mu)$. *Phys. Rev. Lett.*, 115(11):111803, 2015. [Erratum: *Phys. Rev. Lett.* 115, no. 15, 159901 (2015)].
- [16] Christopher J Monahan, Heechang Na, Chris M Bouchard, G Peter Lepage, and Junko Shigemitsu. $B_s \rightarrow D_s \ell \nu$ Form Factors and the Fragmentation Fraction Ratio f_s/f_d . 2017.
- [17] Wolfgang Altmannshofer, Peter Stangl, and David M. Straub. Interpreting Hints for Lepton Flavor Universality Violation. 2017.
- [18] Matthew D. Schwartz. *Quantum Field Theory and the Standard Model*. Cambridge University Press, 2014.
- [19] I.S. Altarev, Yu.V. Borisov, N.V. Borovikova, S.N. Ivanov, E.A. Kolomensky, M.S. Lasakov, V.M. Lobashev, V.A. Nazarenko, A.N. Pirozhkov, A.P. Serebrov, Yu.V. Sobolev, E.V. Shulgina, and A.I. Yegorov. New measurement of the electric dipole moment of the neutron. *Physics Letters B*, 276(1):242 – 246, 1992.
- [20] David J. Gross and Frank Wilczek. Ultraviolet behavior of non-abelian gauge theories. *Phys. Rev. Lett.*, 30:1343–1346, Jun 1973.
- [21] Stefan Scherer. Introduction to chiral perturbation theory. *Adv. Nucl. Phys.*, 27:277, 2003. [277(2002)].
- [22] S. Fubini and G. Furlan. Renormalization effects for partially conserved currents. *Physics Physique Fizika*, 1(4):229–247, 1965.
- [23] C. McNeile, A. Bazavov, C. T. H. Davies, R. J. Dowdall, K. Hornbostel, G. P. Lepage, and H. D. Trottier. Direct determination of the strange and light quark condensates from full lattice qcd. *Phys. Rev. D*, 87:034503, Feb 2013.

- [24] Richard F. Lebed and Mahiko Suzuki. Current algebra and the Ademollo-Gatto theorem in spin flavor symmetry of heavy quarks. *Phys. Rev.*, D44:829–836, 1991.
- [25] Adam F. Falk and Matthias Neubert. Second order power corrections in the heavy quark effective theory. 1. Formalism and meson form-factors. *Phys. Rev.*, D47:2965–2981, 1993.
- [26] Leslie L. Foldy and Siegfried A. Wouthuysen. On the dirac theory of spin 1/2 particles and its non-relativistic limit. *Phys. Rev.*, 78:29–36, Apr 1950.
- [27] G. Peter Lepage, Lorenzo Magnea, Charles Nakhleh, Ulrika Magnea, and Kent Hornbostel. Improved nonrelativistic QCD for heavy quark physics. *Phys. Rev.*, D46:4052–4067, 1992.
- [28] G. P. Lepage. Lattice QCD for novices. In *Strong interactions at low and intermediate energies. Proceedings, 13th Annual Hampton University Graduate Studies, HUGS'98, Newport News, USA, May 26-June 12, 1998*, pages 49–90, 1998.
- [29] G. Munster and M. Walzl. Lattice gauge theory: A Short primer. In *Phenomenology of gauge interactions. Proceedings, Summer School, Zuoz, Switzerland, August 13-19, 2000*, pages 127–160, 2000.
- [30] Thomas DeGrand and Carleton E. Detar. *Lattice methods for quantum chromodynamics*. 2006.
- [31] Karl Jansen. Domain wall fermions and chiral gauge theories. *Phys. Rept.*, 273:1–54, 1996.
- [32] R. Narayanan. Tata lectures on overlap fermions. 2011.
- [33] E. Follana, Q. Mason, C. Davies, K. Hornbostel, G. P. Lepage, J. Shigemitsu, H. Trottier, and K. Wong. Highly improved staggered quarks on the lattice, with applications to charm physics. *Phys. Rev.*, D75:054502, 2007.
- [34] Michael E. Peskin and Daniel V. Schroeder. *An Introduction to quantum field theory*. 1995.
- [35] A. Bazavov et al. Lattice QCD ensembles with four flavors of highly improved staggered quarks. *Phys. Rev.*, D87(5):054505, 2013.

- [36] G.P.Lepage. Corrfitter: <https://github.com/gplepage/corrfitter>, 2012.
- [37] B. Colquhoun, C. T. H. Davies, R. J. Dowdall, J. Kettle, J. Koponen, G. P. Lepage, and A. T. Lytle. B-meson decay constants: a more complete picture from full lattice QCD. *Phys. Rev.*, D91(11):114509, 2015.